Use Authorization

In presenting this thesis in partial fulfillment of the requirements for an advanced degree at Idaho State University, I agree that the Library shall make it freely available for inspection. I further state that permission to download and/or print my thesis for scholarly purposes may be granted by the Dean of the Graduate School, Dean of my academic division, or by the University Librarian. It is understood that any copying or publication of this thesis for financial gain shall not be allowed without my written permission.

Signature: ______________________________

Eric S. Krage

Date: ______________________________

Evaluation of ^{90}Sr Intravenously Injected

Non-Human Primate Using ICRP 78 Model

By

Eric S. Krage

A thesis

submitted in partial fulfillment

of the requirements for the degree of

Master of Science in the Department of Nuclear Engineering and Health Physics

Idaho State University

Spring 2014

To the Graduate Faculty:

The members of the committee appointed to examine the thesis of Eric S. Krage find it satisfactory and recommend that it be accepted.

Dr. Richard R. Brey

Major Advisor

Dr. Jason Harris

Committee Member

Dr. Rene Rodriguez

Graduate Faculty Representative

ACKNOWLEDGEMENTS

I would like to thank my parents Steve and Veronica Krage, extended family and friends for always being there to encourage me. I would also like to express my appreciation and thanks to my advisor Dr. Richard R. Brey, you have always pushed for me to put forth my best effort and for that I am thankful. I would also like to thank my committee members Dr. Jason T. Harris and Dr. René Rodriguez for assisting me and serving on my committee.

Success is not final, failure is not fatal: it is the courage to continue that counts.

Winston Churchill

TABLE OF CONTENTS

LIST OF FIGURES

LIST OF TABLES

ABSTRACT

This study evaluates the ICRP 78 ^{90}Sr hermaphrodite model and its ability to predict the injected activity, and more thoroughly define the activity residing in the skeleton of rhesus monkeys. The data from the skeletal analysis at sacrifice of male and female groups of monkeys are combined to create better profiles of the activity residing in the skeleton. This data along with whole body counts and whole blood analyses was used to optimize the biokinetic parameters using the Integrated Modules for Bioassay Analysis (IMBA) /Weighted Likelihood Monte-Carlo Sampling (WeLMoS) tool to better predict the Intake and fit the bioassay data. The default parameters prediction of the activity in skeleton for both the male and female cohort over predicted the activity in skeleton by as much as 180%. To improve the fit and the predictive capabilities of the model, a Monte Carlo sampling method (WeLMoS) was used to vary the default parameters, producing an improved model fit with the optimized model parameters. The optimized model obtained for the male and female cohorts was then tested on monkeys in the study not used to generate the model. From the evaluation of the optimized parameters the ability to predict the activity in skeleton improved to within 50% of the measured values and the predictive capability of the intake improved to within 40% for most cases tested. The results suggest that the modified transfer rates could be used as default parameters for which further biokinetic modeling is completed using non-human primates as human surrogates.

Chapter 1 INTRODUCTION

1.1 Problem Statement

Strontium is found in nature as a soft metal; radioactive ^{90}Sr is an anthropogenic nuclide generated as a byproduct of nuclear fission reactions (EPA, 2012). The radioactive progeny is purely a byproduct of the fission process, largely dispersed in the 1950s and 1960s owing to atmospheric testing of nuclear weapons. From its initial introduction into the environment it has since been slowly decaying with a half life of 28.79 years. Levels from current testing show that the current abundance of ^{90}Sr in the environment is very low. Two surveys have reported the strontium content in urban air to range from 4 to 100 ng/m^3 and average 20 ng/m^3 (Dzubay, 1975). Concentrations in Illinois were measured to be between 0.9 to 4.8 ng/m^3 between 1985 and 1988 for naturally occurring strontium (Sweet, 1993). The concentrations of strontium in the free air are generally higher near coal fire plants, where strontium is a gaseous product released within the stack emissions (ATSDR, 2004).

The alkaline earth element strontium follows the calcium pathway in the body but exhibits different transfer rates. Both Sr and Ca have similar skeletal uptake and distribution at early times post injection. Within a few months nearly all the total-body activity is associated with bone compartments (ICRP, Age-dependent dose to members of the public from intake of radionclides: part 2, ingestion dose coefficients, 1993). Since strontium is taken up into the bone, the bone itself and nearby soft tissues may be damaged by the cumulative exposure over time. The most detrimental effect takes place within the red bone marrow effecting the production of healthy red blood cells and bone regeneration.

The activity entering through the respiratory tract or gastrointestinal tract is ultimately transferred to the blood and is retained by bone and soft tissues. The rapidly exchangeable activity then is recirculated throughout the body by the blood and is partially excreted in the urine and feces (ICRP, 69, 1995a). Over time the rapidly exchangeable activity is transferred into the bone surfaces and finally to the non-exchangeable bone volume. The ICRP 1990 model (Figure 1.1) is intended to provide reasonably accurate predictions of the time dependent activity on bone surfaces and within the bone volume, as well as rates of excretion after transfer into systemic body fluids for strontium isotopes.

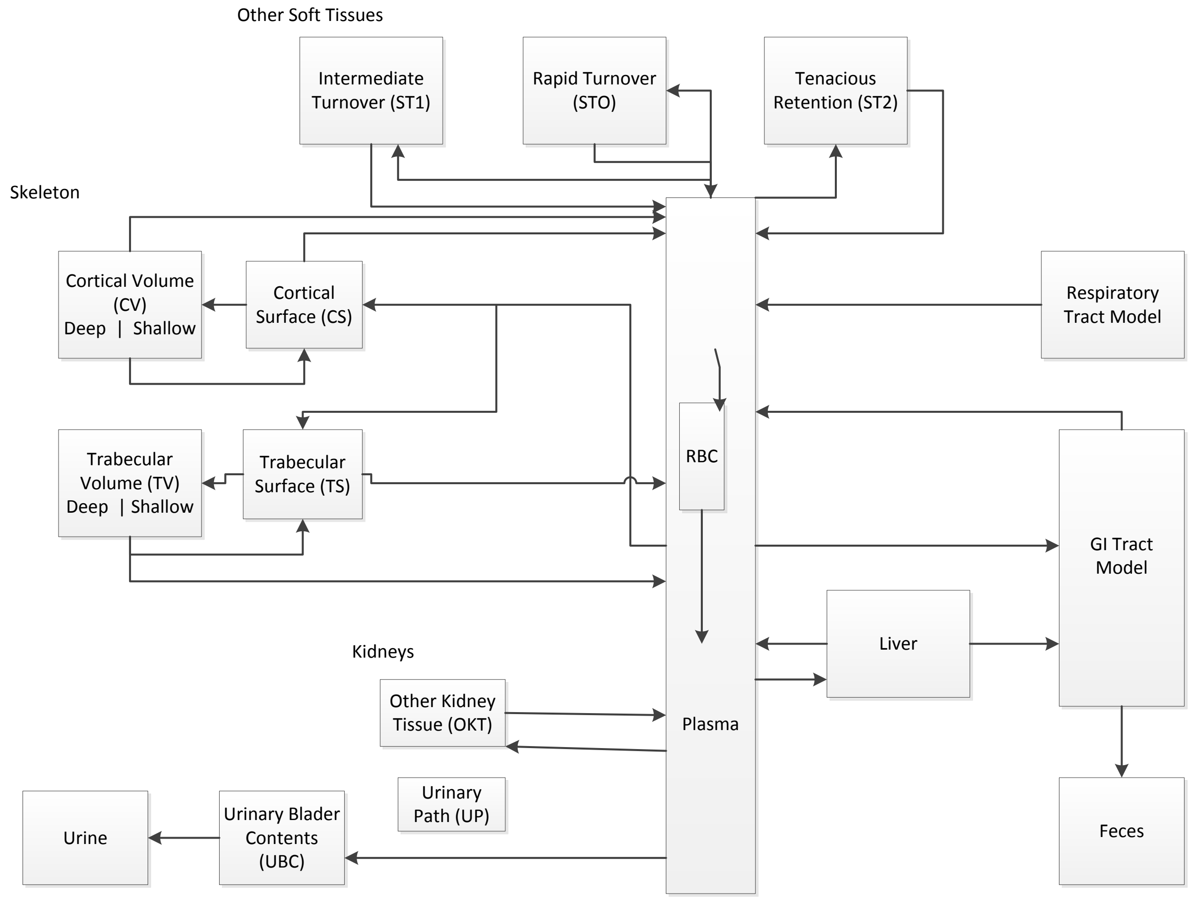

Figure 1. 1 Compartmental Model for Ca-Like Elements "Strontium". (ICRP 1990)

Rhesus macaque monkeys are one of the most extensively studied nonhuman primates and have a broad geographic distribution second only to humans. Because of rhesus monkeys anatomical and physiological closeness to humans, the relative ease at which they can be maintained and bred in captivity, and the available supply from India, Rhesus macaques have long been the non-human primate of choice on which to conduct research on human and animal health-related topics (Mitruka, 1976). The rhesus and humans are known to share a common ancestor from 25 million years ago (Gibbs R, 2007). The rhesus macaque genome has a 93% genomic match with that of humans. Because of the rhesus macaques genomic similarities to humans and physiological characteristics, rhesus macaques are one of the best animal test subjects that may be used for biokinetic studies with radionuclides.

1.2 Purpose of the Study

Among the main purposes of this study is to evaluate the uncertainty in the activity of in vivo whole blood measurements. Blood, a liquid tissue composed of approximately 45% cells and 55% fluid plasma, currently serves as the transfer compartment in biokinetic models. Preliminary work suggests that an uncertainty of 5% can be associated with *in vivo* blood measurements of activity. Applying this uncertainty and the non-human primate bioassay data generated form Lawrence Berkeley Laboratory from 1959 through 1982 by Durbin et al. the biokinetic model of ^{90}Sr was analyzed. A group of male and female monkeys injected with the same activity is used to generate a composite data set to evaluate the ^{90}Sr biokinetic model. The composite data set is generated by combining all data available from a set of monkeys' bioassay data in time. Therefor the data set includes: whole blood measurements, whole body counts, and activity of the skeleton at sacrifice. The composite data set generated a more comprehensive set of data to be fit, which is used to predict the initial intake of ^{90}Sr. A secondary goal of this study was to modify the systemic model parameters as appropriate and necessary in an effort to optimize the predictive capabilities of the model. The improved model parameters were also independently tested with another set of monkeys not used in the generation of the optimized model.

1.3 Hypothesis Testing

The robustness of the ^{90}Sr systemic model will be evaluated by the following hypotheses:

$H_{1,0}$: *The ICRP Report No. 78 systemic model for* ^{90}Sr *will not accurately predict the intake from composited primate bioassay data.*

$H_{1,A}$: *The ICRP Report No. 78 systemic model for* ^{90}Sr *does accurately predict the intake from composited primate bioassay data.*

The null hypothesis will be accepted if the predicted and injected Sr^{90} activities are within 10% of one another. In the event that a larger deviation occurs, the null hypothesis will be rejected in favor of the alternate hypothesis. Support of the null hypothesis suggests that the intake prediction cannot be scrupulously predicted by the default model parameters.

$H_{2,0}$: *Default transfer rates as specified by ICRP No. 78 cannot be altered to improve the predicted composited skeletal bioassay data of* ^{90}Sr *in Male and Female Macaque monkeys.*

$H_{2,A}$: *Default transfer rates as specified by ICRP No. 78 can be altered to improve the predicted composited skeletal bioassay data of* ^{90}Sr *in Male and Female Macaque monkeys.*

The null hypothesis will be accepted if the predicted and injected ^{90}Sr activities are not 10% more accurate than the default prediction. In the event a smaller deviation occurs the null hypothesis will be rejected in favor of the alternate hypothesis. The acceptance of the alternate hypothesis suggests that the skeletal prediction cannot be accurately predicted by the current model.

$H_{3,0}$: Modified transfer rates as specified by this study cannot be used to predict the injected activity of subjects with similar injected activities.

$H_{3,A}$: Modified transfer rates as specified by this study can be used to predict the injected activity of subjects with similar injected activities.

The null hypothesis will be accepted if the predicted and injected ^{90}Sr activities are not 10% more accurate than the default prediction. In the event a smaller deviation occurs the null hypothesis will be rejected in favor of the alternate hypothesis. Support of the alternate hypothesis suggests that the intake prediction cannot be improved by the current model.

Chapter 2 BACKGROUND

2.1 Characteristics of Strontium-90

Strontium-90 is of radiological concern due to the energy of its radiation, relatively long half-life, and high yield in the fission process. The ease of strontium's mobility through the environment and its radiological properties lended itself to be classified early in its discovery as one of the most hazardous nuclear fission byproducts. Strontium-90 is produced in the fission process with a yield of three to four percent and also introduced into the environment by nuclear weapons tests (Glasstone & Dolan, 1977). The radiological properties of ^{90}Sr is found to have a half-life of 28.79 years and upon its decay undergoes isobaric transition emitting a particle with an average energy of 0.2 MeV. The decay product ^{90}Y which is in secular equilibrium with ^{90}Sr also undergoes isobaric transition ultimately emitting a beta particle of 2.28 MeV (max) and decays to stable ^{90}Zr with a halftime of 64.10 hours Figure 2.1.

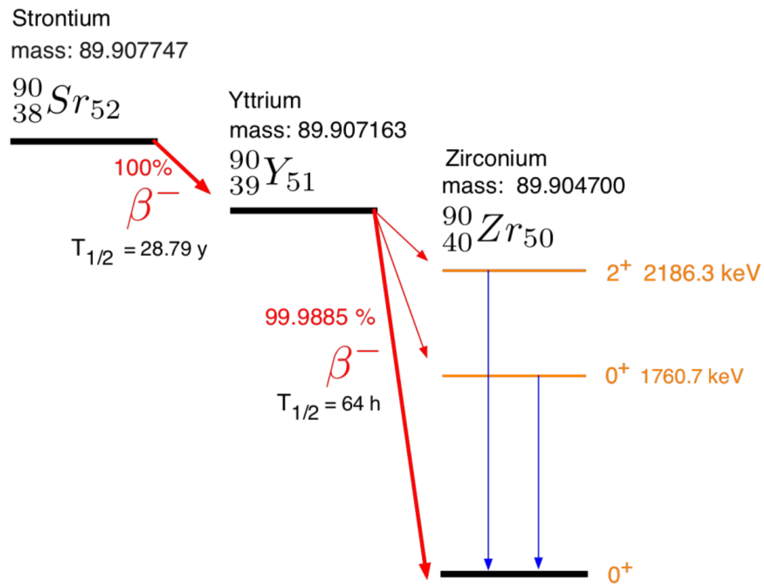

Figure 2.1: ^{90}Sr Radioactive decay scheme

2.2 Strontium Biology

The distribution of absorbed strontium in the human body is similar to that of calcium, with approximately 99% of the total body burden being ultimately found in the skeleton (ICRP, 1993). Pathways to absorption include: ingestion, inhalation, and absorption through the skin via direct absorption or through a superficial wound. According to studies of non-radioactive strontium humans absorb some 11 to 30% of the strontium ingested (WHO, 2010). An age dependent absorption rate was present by which younger rats had a higher absorption (Taylor D, 1962). This was experienced mainly by an increased gastrointestinal absorption rate; although, age dependent gastrointestinal absorption into the body through the ingestion pathway has not been observed in humans. The inhalation pathway is more complex and depends mainly on the chemical species, and particle size of the strontium. The chemical form and size in which strontium particles are usually found has been used to determine its solubility class: days, weeks, or years (D, W, S), which in turn helps one to determine how long it takes the strontium to be absorbed into the body. A competing pulmonary clearance process to absorption is the phagocytosis of foreign particles by alveolar macrophages and their subsequent removal either up the ciliary escalator or by entrance into the lymphatic system (Cember H, 2009). The dermal absorption of strontium is known to be slow through direct means. Wound absorption appears to be dependent on the physical aspects of the wound itself and the chemical species of the strontium (NCRP, 2006).

Strontium, once in the body, can act as an imperfect surrogate for calcium; the distribution of absorbed strontium mimics that of calcium and strontium can exchange with calcium in the bone (ATSDR, 2004). Strontium distributes relatively uniformly within the bone volume, where it exchanges with calcium hydroxyapatite. The strontium to calcium concentration ratio in bone increases with age from $3x10^{-4}$ at birth to $5x10^{-4}$ in adults (Tanaka G, 1981). This ratio is shown to be approximately 10 to 20% higher in cortical bone than trabecular bone.

Once the initial unabsorbed strontium exits the body through excretion, the only means of clearance is the exchange of strontium from the bone to the blood. As strontium exchanges with calcium in the blood, it can be circulated throughout the biokinetic system and be excreted or reabsorbed by the bone. The long term elimination of strontium (i.e. the biological half time) from humans in the Techa River area was reported to be 28 and 16 years for males and females, respectively. The difference in these elimination rates was mainly due to a pronounced increase blood resorption rate in females after menopause (Tolstykh EI, 2011). These estimates of the long term elimination from the body reflect primarily the storage of strontium in bone and its slow recirculation back into the blood.

While examining short periods after exposure, elimination rates appear to be faster, this is thought to be due to soft tissue elimination. Other contributors to this route can be attributed to the rapidly exchangeable bone volume. Considering the rapidly exchangeable bone volume, it appears that strontium follows the calcium pathway, it is either taken up rapidly by new bone formation or phagocytized in the extracellular fluid and excreted (Fraser R, 1960).

2.3 Internal Dosimetry of ^{90}Sr

Determination of the radiation dose and related health risks due to an internal uptake is a complicated task. Knowledge of the number of transformations and energy per transformation is essential to determining the absorbed energy in the target tissues. This type of information is valuable for medical, regulatory, and public health purposes. Assessing dose from an internal exposure is much more complex than that of the external exposure (J & P, 2008).

As recommended by ICRP publications, the first step in assessing internal dose is to evaluate the distribution and retention of a radionuclide in the body and organs through the use of biokinetic models (ICRP 1993 DOE-STD-1121-98, Section 7,). Essential to all calculations of dose for long-lived radionuclides like ^{90}Sr deposited in tissue is knowledge of the kinetics of retention; because the rate of elimination frequently has much more influence on dose as does the physical half-life. Using these kinetic models; the total number of disintegrations occurring in each source organ or tissue can be calculated. A dosimetric model is used to calculate the mean absorbed dose, D_T, to target organs; a result of radioactive decay and the associated decay energies from each source region. The type of radiation is taken into account by applying the radiation weighting factor (W_R) and hence this value correlates to the detrimental stochastic health effects. The equivalent dose in the tissue or organ (T) due to a given radiation type (R) is represented by the following:

$$H_{T,R} = W_R * D_{T,R} \tag{2.1}$$

The total equivalent dose, H_T to an organ or tissue is therefore represented by the sum of all radiation types $H_{T,R}$:

$$H_T = \sum_R H_{T,R} \tag{2.2}$$

The application of the tissue weighting factor (W_T) to account for the contribution of individual organs and tissues overall risk of deleterious effects the typical end point is estimating risks associated with an intake of radioactive material. The effective dose (E) then may be calculated in the tissue or organ (T) by the following expression.

$$E(Sv) = \sum_T W_T * H_T \tag{2.3}$$

2.4 Systemic Biokinetic Models for Alkaline Earth Elements “Sr”

Strontium is a chemical and physiological analogue of calcium but has different biokinetics from calcium. Biological hydroxyapatite crystals of the bone discriminate between these elements. These biokinetics have been studied in human subjects and laboratory animals. These studies clarify the behavior of strontium at early times after intake but are considered by many to be lacking in long term data. The structure of the model for systematic strontium is similar to that of other calcium chemical congeners as seen in Figure 2.2. This simplification includes eliminating the effect of the transfer of strontium between the blood and blood plasma which is a simplified model for bone-volume seekers. Soft tissues are all inclusive into three “other-tissue” compartments: ST0, ST1, and ST2; corresponding to rapid, intermediate, and slow exchange of activity with blood respectively.

The exchange mechanism between these components is the blood compartment. The blood is treated as a uniformly mixed pool that exchanges activity with soft tissues and the bone surfaces. The divisions of the soft tissues are classified by their three respective transfer rates with the blood. The liver and kidney are lumped into the model in these tissues and are not treated as exclusive compartments. The bone is divided into two types cortical and trabecular bone, and further subdivided into bone surfaces and bone volumes. The bone volume is viewed as consisting of two pools; one that exchanges with activity in bone surface for a period of weeks or months, a second, non-exchangeable pool by which activity is removed solely by the bone restructuring process. Activity depositing in the skeleton is assigned to bone surfaces; over a period of days a portion of the activity on bone surfaces moves to exchangeable bone-volume while the remainder returns to the blood plasma. Activity leaves the exchangeable bone-volume over a period of months, with part of the activity moving to bone surfaces and the rest to non-exchangeable bone-volume. The rate of removal from non-exchangeable bone volume is assumed to be the rate of bone turnover, with different turnover rates applying to cortical and trabecular bone. The only means by which strontium is assumed to leave the body is by fecal and urinary excretion. The transfer rates for this model are represented by Table 2. 1 and are in units of inverse days (d^{-1}).

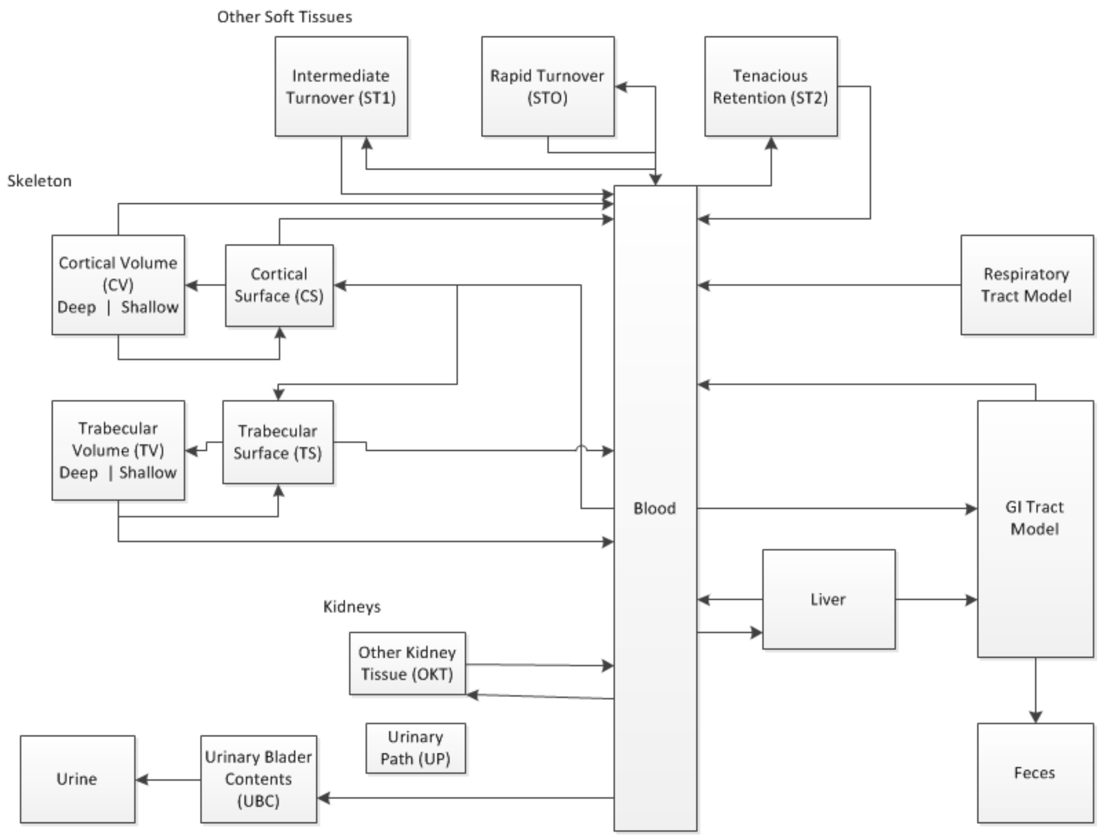

Figure 2.2 Strontium Biokinetic Model

Table 2.1: Strontium Transfer Parameters

Starting Compartment	Ending Compartment	Default Transfer Rate (d^{-1})
BLOOD	ST0	7.50E+00
BLOOD	ST1	1.50E+00
BLOOD	ST2	3.00E-03
BLOOD	CORTICAL SURFACE	1.67E+00
BLOOD	TRABECULAR SURFACE	2.08E+00
BLOOD	RC CONTENTS	1.16E-01
BLOOD	URIN BLADDER CONT	5.78E-01
CORTICAL SURFACE	EXCH CORT VOL	1.16E-01
CORTICAL SURFACE	BLOOD	5.78E-01
NONEX CORT VOL	BLOOD	8.21E-05
EXCH CORT VOL	CORTICAL SURFACE	4.30E-03
EXCH CORT VOL	NONEX CORT VOL	4.30E-03
TRABECULAR SURF	EXCH TRAB VOL	1.16E-01
TRABECULAR SURF	BLOOD	8.21E-04
NONEX TRAB VOL	BLOOD	4.93E-04
EXCH TRAB VOL	TRABECULAR SURFACE	4.30E-03
EXCH TRAB VOL	NONEXCH TRAB VOL	4.30E-03
ST0	BLOOD	2.50E+00
ST1	BLOOD	1.16E-01
ST2	BLOOD	3.80E-04
URIN BLADDER CONT	URINE	1.20E+01

2.5 ICRP Systemic Model Development

The development of the systemic model for ^{90}Sr relies heavily on the environmental data to represent physiological mechanisms. The quality of the experimental data is reflected in the accuracy of the model. Also, the data used to validate the model is indicative of the quality of the model itself.

An interest in understanding ^{90}Sr biokinetics began in the 1950s after large scale atmospheric nuclear weapons tests were conducted; resulting in the dispersal of large quantities of strontium in the environment (US EPA, 2012). The data from the atmospheric testing and animal studies were used for the development of the ICRP strontium biokinetic model (Leggett, 1992). Strontium biokinetics from food, milk, and other contaminated items due to the fallout from the nuclear tests are complicated but give good general knowledge. Interpretation of this environmental data is further complicated by the fact that measured skeletal burdens were measured over an extended period and the ^{90}Sr intake function was not well established (Tolstykh, 2011). The studies do however provide substantial evidence that once ^{90}Sr is absorbed into the blood stream, it accumulates there and resides for a long period of time (Synhaeve N, 2011).

There are many proposed alternate models describing the biokinetics of strontium and other nuclides (Hollrigl V, 2002). The problem with the proposed changes is that they are using the same dataset with which that model was created. Albeit the some data set represents human subjects, they were not experimentally controlled cases of uptake. This problem with circular logic apparently, has not lead the ICRP from changing the model. ICRP publication 67 models were assumed to provide a reasonable representation of the distribution and retention of strontium and radium in the body for all age groups. ICRP points out the large uncertainty of these models; noting that age and sex specific skeletal retention may deviate from the central model predictions. This deviation needs to be better understood to more precisely determine the difference in male and female cases.

2.6 Validation of ICRP Systemic ^{90}Sr Model

To validate the ICRP biokinetic models for strontium many studies have been reviewed including animal investigations, reviews of chemical congener data, or data collected from humans that accidentally ingested ^{90}Sr. When mice drank water containing ^{90}Sr, it was observed that a vast majority of the long term assimilated ^{90}Sr was located in the bones, in similar accounts as predicted by the default strontium model (Synhaeve N, 2011). Most recently acquired data show acceptable agreement with the ICRP 67 predictions for ^{90}Sr retention in skeleton, although some authors have suggested that the model needs to account for both age and gender differences in strontium metabolism (Sagine NB, 2003). Recent studies also suggest that ^{90}Sr biokinetics are strongly dependent on both age and gender (Synhaeve N, 2011) (Leggett, 1992) (Sagine NB, 2003). The rate of ^{90}Sr elimination appears to be strongly dependent on the rate of bone regeneration, which was seen with advancing age during evaluation of the Techa River cohort (Tolstykh EI, 2011). Mice studies demonstrate a significant difference in the activity residing in the skeleton based on age and sex. This study provided further evidence that uptake of ^{90}Sr is reduced in adults compared to juveniles (Tolstykh EI, 2011). It has been thought that this observation is likely due to difference in bone remodeling rates and potentially osteoporosis.

It should be noted that many alteration and or substitutions have been proposed to the ICRP biokinetic models (Tolstykh EI, 2011) (Tolstykh & Degteva MO) (Li BO Wei, 2006). Evaluating the Techa River cohort of human data, Shangina found that the ICRP model structure was adequate to describe ^{90}Sr retention in bone, but that the model could be improved upon. Suggestions for improvement include the simplification of the biokinetic model by reducing the number of compartments and implementing a multi-exponential function to predict strontium retention or by the ability to write switch equations to modify the exponentials to account for things such as age and gender (Malinovsky G, 2013). The switching equations of n variable is a function that assigns to each a binary sequence of length (n) the number 0 or 1 signifying that the equation is either active or inactive. When used with other biokinetic equations more complex parameters can be taken into account and a streamlined linked model for all humans can be derived.

Chapter 3 DATA COLLECTION AND MEASUREMENTS

3.1 Laboratory Experiment Outline

Between 1963 and 1982, a series of studies were conducted at the Division of Research Medicine and Radiation Biophysics in affiliation with Lawrence Berkley Laboratory. The studies were conducted to obtain ^{90}Sr biological data as a basis to improve human biokinetic models. Previous animal studies mainly focused on rats. The lifespan of rats was postulated to be too short for a complete understanding of what might occur in humans, especially for long lived bone-seeking radionuclides like ^{90}Sr (Durbin PW, Collected original data on distribution of 90Sr in bones of monkeys, 1993a). Pilot studies suggest that biokinetic data collected from macaque monkeys would serve as an acceptable surrogate for the development of a human biokinetic model for bone seeking radionuclides (Durbin PW, Collected original data on distribution of 90Sr in bones of monkeys, 1993a).

Using monkeys as research subjects has a unique history within the topic of animals in science. As the animals most closely related to humans, phylogenetically, physiologically, and anatomically; they have important uses in research (IPS, 1995-2014). The use of primates in biomedical research has led to numerous medical advances and an understanding of biokinetic modeling with radionuclides. Although primates are available for research, there are pressures not to use them, including the high cost of maintenance of a program and their endangered status in the wild. Their close genetic relationship to humans, which makes them the appropriate surrogate for human health research, also gives rise to ethical concerns. The U. S. Federal government owns or supports approximately one thousand monkeys for research. (National, Research, & Council, 1997).

A total of 76 monkeys were exposed to ^{90}Sr in the Durbin study. The study included exposure by four modes: intravenous injection, intramuscular injection, intraperitoneal, and a feeding regime. A group of male and female monkeys were subsequently administered a one-time injection of 205. 29 uCi $^{90}Sr(NO_3)_2$ obtained from Oakridge National Laboratory. The stock solution was prepared by diluting 3,700 Bq-ml^{-1} in 2N HCl and stored in a refrigerator. The required injection volume was diluted in sodium citrate (30 mg-ml^{-1}) in a serum bottle. The desired volume for each monkey (1 to 5ml) was drawn into a glass syringe; after 1967, syringes were weighed filled and empty for a more accurate measurement of the amount delivered. An additional syringe containing a measured volume (or mass) of each solution prepared for injections was expressed into a volumetric flask containing 2N HNO_3 to provide counting standards for a monkey injected on a particular day. The quantity of ^{90}Sr injected into each monkey was inferred from three separate calibrations of these counting standards: (i) measurement of total beta activity with a calibrated thin-window GM counter, (ii) measurement of separated ^{90}Y daughter by an outside contractor, (iii) measurements of bremsstrahlung with a pair of calibrated thin NaI(Tl) crystals (Durbin PW, Collected original data on ^{90} Sr in plasma, whole body and excreta of monkeys, 1993b). The intravenous (i.v.) injections were made into superficial veins of the calf and ankle, while intramuscular injections were made into the thickest part of the thigh.

3.2 Excretion Collection

The excreta from the subjects were collected from all monkeys daily or every other day for the first two weeks after the ^{90}Sr injection. During that time, urine and feces were collected separately, except a few monkeys early in the study where they were not separated. After the initial two weeks, samples were collected twice a week for six to twelve months. Subsequently two week time intervals of collection were combined 4 to 6 times a year until sacrifice.

3.3 Blood Sampling Procedures

Blood samples for the subjects were drawn from superficial leg veins at various frequencies. Frequent early blood samples were taken from some animals in the study to help define the kinetic pattern of clearance. When obtaining more frequent blood samples small aliquots of blood (1 to 3 ml to minimize blood loss) were drawn several times in the first 6 to 8 hours, twice daily for 3 or 4 days, once daily for about two weeks, and at succeedingly longer intervals thereafter. Blood was drawn from every animal in the colony at least twice a year for hematological examination. When blood was drawn at the less frequent intervals, approximately 3 to 10ml of sample volume was obtained depending on the subjects mass. The blood was collected in syringes that were pre-weighed and post-weighed after dispensing it to obtain the sample weight.

3.4 Whole Body Counting

During the investigation *in vivo* measurements of strontium retention (whole body counts) were conducted at regular intervals. The whole body counts were initiated half-way through the study once a whole body counting system was made available, so there is a lack of data early on for some of the subjects. Once the whole body counting study was initiated monkeys were tested at minimum bi-annually. Additionally, if monkeys had to be tranquilized for other reasons, they were also whole body counted.

Concurrently with every whole body counting procedure, the animals were tranquilized and weighed. The monkey was then placed into a carrying box in a curled up position as shown in Figure 3.1 and held in place by packaging material Figure 3.2. The reason for the packing in the tube was to generate a similar geometry for each subject tested. The facility used for the counting setup was a low background room. The facility utilized a large NaI (Tl) detector (24-cm dia. by 10-cm thick) active surface area. The room was set up to allow for the precise position of the detector with respect to the counting subject. During counting the crystal was positioned 1 meter from the animal setup. The cage was positioned such that the central point of the box-lid was directly below the mid-point of the crystal face. This position allowed for maximum counting efficiency as verified with a counting standard designed from another monkey case.

Figure 3.1 Whole Body Counting Geometry

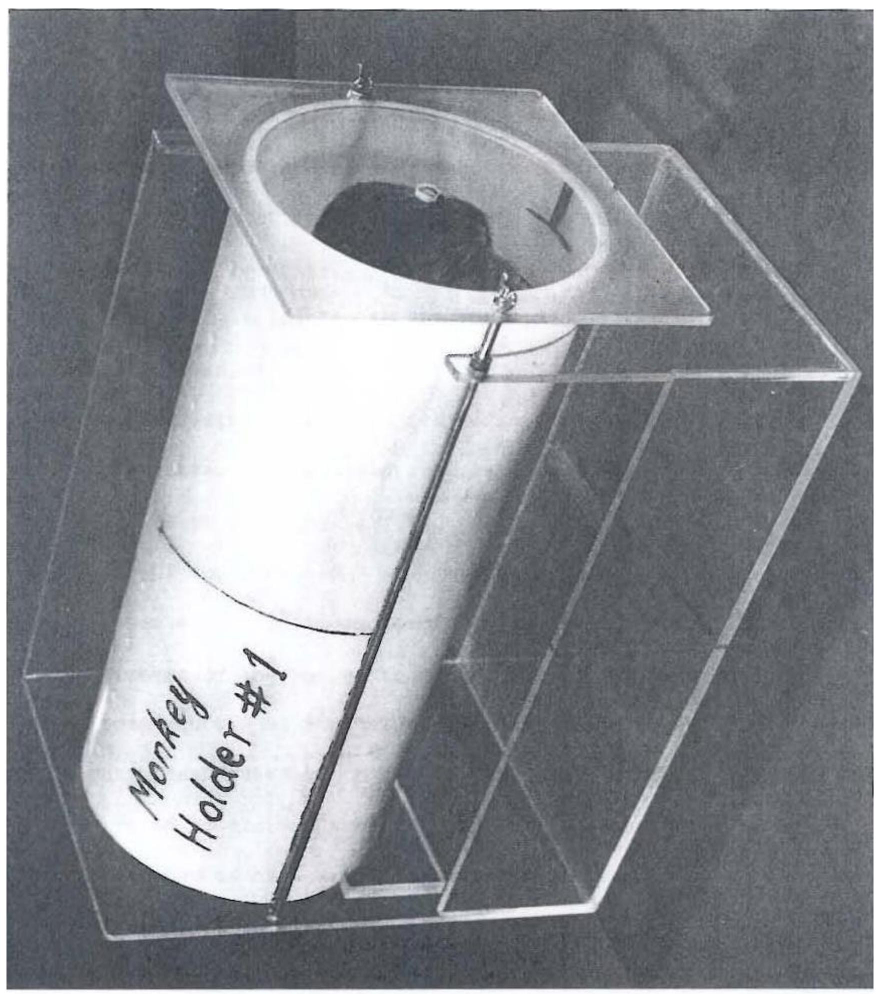

Figure 3.2 Whole Body Counting Set up

3.5 Autopsy Procedures

The subjects were sacrificed for further analysis if they became ill or at the preplanned time. This was done with an overdose of sedative from 1 to 5,700-days post injection. Following the sacrifice of animal, an autopsy was performed. During the autopsy, the thoracic organs and abdominal organs were removed. The blood pool remaining was removed to the extent. The blood pool was extracted from the inferior vena cave via a catheter. The excess fecal matter was removed from the gastrointestinal tract and added to the final fecal collection. The soft tissue was separated from the skeleton and both compartments massed and dried in an oven at 100 ^{o}C. The bones were disarticulated and any remaining flesh or cartilage removed. The leg in which the injection took place was analyzed separately as a whole prior to this process. The bones after disarticulation were then further subdivided into multiple segments and radioanalyzed.

3.6 Sample Preparation Techniques

After oven drying: blood, bone, excreta, and tissue; samples were heated in a furnace at 500 to 600 ^{o}C until they were further reduced to ash. The total ashed weights of the bones were recorded. Dry-ashed excreta and large soft tissues were digested with concentrated HNO_3, and 30% H_2O_2 to eventually form a carbon free salt. The small ashed samples were further processed by dissolving them in 6N HNO_3 and then they were evaporated onto glass or steel planchets. The larger samples were acidified for a longer period of time to fully digest the salts. The acid in the samples were neutralized by the addition of NH_4OH, evaporated, and ultimalty cooled and weighed.

During analysis of the individual excretion samples, it eventually became inevitable that the activity in the individual samples were below detection capability. The lower activity in the samples was due to the time post injection of ^{90}Sr and the limited initial injected activity (Durbin, 1993). This problem lead to longer collection periods for excreta, increased collection periods to one or two weeks at 6 to 12 months post-injection.

3.7 Bio-Assay Sample Counting

The bioassay samples collected were analyzed by different detection systems throughout the study as better technology was introduced. The detection system as the study started was an in house built GM tube which had a detection efficiency of 37% for a thin film and dropped to 21. 5% for the more massive ashed samples. The three commercial systems used were:

i. Nuclear-Chicago gas flow proportional counter
ii. Nuclear-Chicago 5-cm thick NaI(Tl) detector
iii. Dual NaI (Tl) crystal set up for counting ^{90}Sr / ^{90}Y decay products (Durbin

1993). Over time components of the counting system were upgraded and replaced, but due to the high quality control the replaced parts did not degrade analysis results.

The skeleton of the subjects to undergo analysis were disarticulated and soft tissue removed. The segments were then weighed wet and again after they were ashed for counting. Some soft tissues, fecal, and urine samples after oven drying and dry ashing, needed additional wet digestion with concentrated acid and hydrogen peroxide. These samples were dissolved in 6N HNO_3 to generate fully dissolved homogeneous mixtures. The mixtures were then either prepped for counting in 14-ml test-tubes and counted using a well scintillator, or plated out onto planchets for counting.

To correct for due to self-absorption of the samples, self-absorption correction curves relating the percent transmission of ^{90}Sr / ^{90}Y to dry mass on the planchet were prepared. The curves were prepared using dissolved bone ash or reagent grade $Ca_3(PO)_2$. The self-absorption curve for ^{90}Sr / ^{90}Y in excreta samples was prepared using excreta ash in order to compensate for the presence of the small mass of non-volatile insoluble residue containing little or no radioactivity. The plant diet the monkey was on contributed to a small, but detectable, amount of ^{40}K, which increased the background beta count rate in urine and combined excreta samples. Over the range of dry samples weights of 20 to 200 mg on the planchets, ^{40}K accounted (on the average) for 0.045 to 0.085 counts/min/mg, uncovered or covered with a 64 mg cm^{-2} aluminum filter, respectively. Accounting for these types of error in the activity provided more reliable and robust data to analyze.

Chapter 4 ANALYSIS METHODS

4.1 Using Bioassay Data to Estimate Intake

Bioassay samples and *in vivo* measurements are undertaken to quantify the intake after a potential uptake of radioactive material. The measurement of the radioactivity in the body's organs or in the whole body (in vivo), or measurements in samples of excretion (in vitro), must be interpreted using biokinetic models to quantify the radioactive material taken in to the body. These mathematical biokinetic models describe the translocation, distribution, and elimination of specific radionuclides in specified physical and chemical forms. Most biokinetic models attempt to describe activity in organs and excreta as a function of time following intake, from which a committed effective dose can be calculated using the product of the intake and dose coefficient (Doerfel H, 2006).

An overview of the analytical treatment of models for internal dosimetry is present in Publication 30 (ICRP 1978). However, the method of solving for the activity residing in a particular compartment was limited to the linear flow of activity through the body not allowing feedback (Skrable KW, 1974). Through the years, models have been developed to better represent the biological process and to include recirculation of material through the body before exiting. The advancement of biokinetic models has led to abandoning analytical representations and resorting exclusively to numerical computer calculations to solve the ever increasingly complex models (Polig E, 2001) (Pogliani L, 1996).

To evaluate the ICRP 78 hermaphrodite model, it is assumed that we will evaluate a single intake in which the compartments follow first order kinetics which can be described by a system of linear differential equations. The change in the amount of activity with respect to time shall be equal to the transfer rate matrix multiplied by the individual transfer rates between compartments.

$$\frac{d\boldsymbol{q}}{dt} = \boldsymbol{Rq} \qquad \textbf{(4.1)}$$

Where the constant matrix **R,** is the matrix of transfer rates with elements r_{ij} representing the fractional transfer rate from compartment *j* to compartment *i*. The elements $q_i(t)$ of the "state vector" **q**(t) of the n-compartment system represent the contents of compartment *i* at time *t*. In addition to biological transfer, a radionuclide with decay constant λ disappears with this rate from all compartments. Thus physical decay and biological transfer combined yield:

$$\frac{d\boldsymbol{q}}{dt} = \boldsymbol{Aq}; \;\; \boldsymbol{A} = \boldsymbol{R} - \lambda\boldsymbol{I}; \mathbf{q}(0) = \boldsymbol{q}_0. \qquad \textbf{(4.2)}$$

So that **q** is defined by a set of column vectors and **I** is the n*n identity or unit matrix. Without the loss of generality it is assumed that at time t = 0 and time t_i the state of the system is known to be $\mathbf{q_0}$. This simply means that the calculation starts with known compartment contents. The solutions of equation (4.2) is completely analogous to the one-dimensional case

$$\boldsymbol{q}(t) = e^{At}\boldsymbol{q}_0 \qquad \textbf{(4.3)}$$

where the matrix-exponential e^{At} is a matrix defined by its series expansion:

$$e^{At} = \sum_{i=0}^{\infty} \frac{(\mathbf{A}\boldsymbol{t})^i}{i!};\ \mathbf{A}^0 = \boldsymbol{I} \qquad \textbf{(4.4)}$$

The definition in equation (4.4) is not always useful for a practical calculation because series may converge slowly. Birchall and James derived an algorithm for calculating the exponential based on the above series expansion and combined with a procedure of convergence acceleration (Birchall & James, 1989). The Birchall and James algorithm is what is used by Integrated Model for Bioassay Analysis IMBA and WELMOS to calculate the intake from bioassay data. However, the most common method of calculating the matrix exponential is by using eigenvalues and eigenvectors of $\mathbf{A}^{\mathbf{T}}$.

A theorem of linear algebra states that an n*n matrix **A** with linearly independent set of n eigenvectors can be decomposed by a similarity transformation into

$$\boldsymbol{A} = P\boldsymbol{\Lambda}\boldsymbol{P}^{-1} \qquad \textbf{(4.5)}$$

Where **P** is the matrix who's n columns are formed by the n eigenvectors $\mathbf{p}_i$, $\mathbf{P}^{-1}$ is the inverse of **P**, and Λ is a diagonal matrix formed by the n eigenvalues $\lambda_i, \ldots, \lambda_n$ on the main diagonal and zero everywhere else:

$$\boldsymbol{A} = (\boldsymbol{p_1}, \ldots., \boldsymbol{p_n}) \begin{pmatrix} \boldsymbol{\lambda_1} & \mathbf{0} & \mathbf{0} \\ \mathbf{0} & \ddots & \mathbf{0} \\ \mathbf{0} & \mathbf{0} & \boldsymbol{\lambda_n} \end{pmatrix} (\boldsymbol{p_1}, \ldots., \boldsymbol{p_n})^{-\mathbf{1}} \qquad \textbf{(4.6)}$$

With the eigenvalues and eigenvectors known, all functions of **A** can be calculated easily, because

$$\boldsymbol{A} = P\ F(\boldsymbol{\Lambda})\boldsymbol{P}^{-1} = \ \boldsymbol{P} \begin{pmatrix} \boldsymbol{F}(\boldsymbol{\lambda_1}) & \mathbf{0} & \mathbf{0} \\ \mathbf{0} & \ddots & \mathbf{0} \\ \mathbf{0} & \mathbf{0} & \boldsymbol{F}(\boldsymbol{\lambda_n}) \end{pmatrix} \boldsymbol{P}^{-\mathbf{1}} \qquad \textbf{(4.7)}$$

If $F(A) = e^{At}$:

$$e^{At} = P\begin{pmatrix} e^{\lambda_1 t} & 0 & 0 \\ 0 & \ddots & 0 \\ 0 & 0 & e^{\lambda_n t} \end{pmatrix} P^{-1} \tag{4.8}$$

And if $F(A) = A^{-1}$:

$$A^{-1} = P\begin{pmatrix} \frac{1}{\lambda_1} & 0 & 0 \\ 0 & \ddots & 0 \\ 0 & 0 & \frac{1}{\lambda_n} \end{pmatrix} P^{-1} \tag{4.9}$$

The mathematical routines for calculating eigenvalues and eigenvectors are available in most mathematical software. The special situations of multiple eigenvalues or the case of not having a full set of n linearly independent eigenvectors exists is not discussed. With commonly used biokinetic models for radionuclides and the real numbers associated with the solutions these situations practically never occur.

Considering the solution given using equation 4.3 and 4.8, it is clear that $\lambda_i \leq 0$ for (t) approaching infinity the state vector **q** must remain finite. In cases of a stable element ($\lambda = 0$), one or more eigenvalues may be zero. If, after renumbering, we assume that the first m eigenvalues are zero, then the system settles on a non-zero state vector $\mathbf{q}_\infty$ for (t) going to infinity.

$$q_\infty = Bq_0; B = P\begin{pmatrix} I_m & 0 \\ 0 & 0 \end{pmatrix} P^{-1} \tag{4.10}$$

$\mathbf{I_m}$ is the m*n unit matrix. The eigenvectors in **P** have to be renumbered accordingly. Zero eigenvalues occur if the system has traps, i.e., it contains compartments that are irreversibly connected to their environment (Polig E, 2001).

So, in solving the complex biokinetic systems the intake and or activity in a specific compartment can be calculated using eigenvectors and eigenvalues as well as the series expansion method from Birchall and James (Birchall & James, 1989). This allows for the quick analysis of bioassay data to predict activity and ultimately calculate the dose.

4.2 Uncertainties in Bioassay Measurements

The propagated uncertainty in all measurements and analysis of bioassay data is needed to more accurately predict dose to the subject. Although there are large generalizations made in current biokinetic models, the collective uncertainty in bioassay data should be minimized to allow for a better fit of the data when using the maximum likelihood function. The improved fit of the multiple bioassay data sets will improve the predictive capability of the model. This enables an objective approach to determining whether or not the intake and calculated dose are consistent with the data (Marsh JW, 2008).

The uncertainty in bioassay measurements takes one of two forms (Type A or Type B) of counting errors. The Type A error represents the stochastic nature of radioactive decay measurement error that is associated with the detection of decay events. While Type B errors may be associated with: recovery rate in in-vitro and in-vivo samples, sample size variation, sample counting efficiencies, and variations of material biokinetics (Marsh, 1998). In the literature from Durbin the activity in the blood was given in terms of (%ID) which is the percent of the activity identified in the sample compared to injected activity. To use the blood data, it was necessary to convert this value to the activity in the blood compartment using Equation 4.11. The parameters used in the equation are listed below along with their associated uncertainty in the measurement. To use the data in IMBA-PPAE an error in the overall measurement must be derived which is represented in Equation 4.12 and an example of the propagated error for one component is shown in Equation 4.13.

- $A_{\%}$ = Sample Content square root(%ID)
- A_o = Activity Injected square root(Bq or uCi)
- M_B = Mass of Monkey (±0.005 Kg) (Durbin PW, Collected original data on 90 Sr in plasma, whole body and excreta of monkeys, 1993b)
- M_S = Mass of Sample (±0.005 g) (Durbin PW, Collected original data on distribution of 90Sr in bones of monkeys, 1993a)
- MtBV = Mass of Monkey to Total Blood Volume Conversion Factor (54.1 ± 2.0 ml/Kg) (Gregersen MI, 1959)
- ρB = Mass of Sample to Volume of Sample Conversion Factor (1.0582 ± 0.0027 g/ml) (Ageyama, 2001)

$$Total\ Activity\ In\ Blood\ (TAB) = \frac{A_{\%} * A_o * M_B * MtBV * \rho B}{100 * M_S} \quad \textbf{(4.11)}$$

$$\delta(TAB) = \sqrt{\begin{array}{c}(\delta TAB_{MB})^2 + (\delta TAB_{MtBV})^2 + (\delta TAB_{Ao})^2 + \left(\delta TAB_{\rho B}\right)^2 \\ +(\delta TAB_{A\%})^2 + (\delta TAB_{Ms})^2\end{array}}$$

(4.12)

$$\delta TAB_{M_B} = \left|\frac{\partial TAB}{\partial M_B}\right| * \delta M_B = \left|\frac{A_{\%} * A_0 * MtBV * \rho B}{100 * M_S}\right| * \delta M_B \quad \textbf{(4.13)}$$

4.3 Integrated Modules for Bioassay Analysis (IMBA)

IMBA, the Integrated Module for Bioassay Analysis, is an internal dosimetry suite of software developed by the United Kingdom Health Protection Agency (UK-HPA). The IMBA software under license to Idaho State University by its developers is an extended research edition which allows more customizability. The IMBA software is capable of calculating activity in organs, and dose due to internally deposited organs due to their translocation kinetics. The biokinetic models of International Council on Radiation Protection (ICRP) and the National Council on Radiation Protection (NCRP) are capable of being incorporated into IMBA software to solve the activity and or dose in a specific organ given a known intake. Alternately, through the analysis of posterior biokinetic data following an intake, the bioassay data can be compared to the mode of uptake, and an estimated intake can be calculated. The advantage of IMBA over hand calculations or other programs is that it allows the analysis of multiple and different bioassay samples, either individually or simultaneously, to predict the intake. The calculation of predicted bioassay quantities, Intake and doses can be calculated for up to 10 individual intake regimens, determined by the duration of the intake either acute or chronic, time of intake and route of entry (i.e. absorption, ingestion, inhalation or injection) (Birchall A, 2007).

The IMBA software under license to Idaho State University is an extended research edition, known as IMBA Professional Plus Academic Edition (IMBA-PPAE) (Version 4.1.49). This extended version of the software package allows a Bayesian fitting methodology that enables the calculation of intakes from bioassay analysis. Furthermore, IMBA-PPAE allows the user to operate in future model mode. Future mode allows the creation of custom biokinetic models and the ability to add, subtract, and change model parameters of current ICRP, NCRP, or custom models.

The ICRP-78 strontium model for hermaphrodites was use due to its applicability to either sex in the case of the two cohorts of monkeys studied. Subsequently the ICRP model was designed and input into the IMBA-PPAE biokinetic model builder. To calculate the retention functions of the group, a composite of the model monkeys were generated. The composite retention functions were made by combining all data for the male and female cohorts. When building the composite dataset, individual monkey data that overlapped on the same day was averaged. Once the data was composited, and after being organized into an appropriate IMBA input file the retention for the selected compartments was analyzed by inputting the known intake, and calculating the activity based on the ICRP model. The difference was then calculated and compared to the actual measured data to make a judgment as to the accuracy of the prediction.

The IMBA-PPAE software utilized the maximum likelihood fitting method to determine the best fit of the retention curve, resulting in the calculation of the best estimate of the intake given a set of bioassay data as previously discussed. Using the maximum likelihood method, IMBA-PPAE calculates the best intake (I) from the bioassay data (m_it_i) such that the product of (I) and f(t) best fit the data, were f(t) represents the fitted retention function of the bioassay data (James 2005). The difference between the predicted intake and the known intake was minimized. The relative goodness of fit using the maximum likelihood curve compared to the predicted data and systemic model was determined by calculating the chi-squared (χ^2) as outlined in the following section.

4.4 IMBA Statistics

IMBA-PPAE utilizes the chi-squared statistic to evaluate the "goodness of fit" of biokinetic models to bioassay data. The chi-square statistic (χ^2) is a measure of the difference between the values in the measured time dependent series data and that of the model predicted curve. If each measurement is assumed to have a normal distribution, the value of χ^2 is calculated as follows (Doerfel H, 2006).

$$\chi^2 = \sum\left(\frac{(Im(t)-M(t))^2}{M(t)}\right) \tag{4.14}$$

Where the product $I_m(t)$ is the predicted value. In IMBA, when the predicted values are sent to multiple types of bioassay data simultaneously, the overall χ^2 is equal to the sum of the calculated χ^2 for each data set. When evaluating Equation 4.14 for the chi-squared statistic, it becomes evident that a value of zero would indicate a perfect fit. In this data set, it is highly improbable that such a fit will be achieved due to the compositing of the data set and because of the uncertainties related with the data. However, a decrease in the χ^2 statistic when comparing he modified model parameter and the default model, may indicate an improved model fit. Inversely if the model predictions inadequately describe the measured data, the calculated value of the chi-square statistic will increase from the default model as well as the theoretical value of chi-square distribution.

4.5 IMBA Uncertainty Analyzer

The use of the integrated model for bioassay analysis uncertainty analyzer (IMBA-UA) standalone module provides a method of analyzing bioassay data and calculating the intake and ultimately the dose when the varied parameters are modeled in

IMBA. The IMBA-UA module uses Bayesian statistics to analyze and fit the bioassay data and is a widely used and accepted method in internal dosimetry calculations (Miller G M. H., 2002) (Miller G I. W., 2000). Bayes theory is used to combine a priori knowledge about the value of the intake with the observed bioassay data to produce an *a-priori* posterior probability distribution of the intake (Birchall A, 2007). Where an *apriori* piece of information is known relative to the intake, a Bayesian probability distribution function of the intake can be ascertained and subsequently can be used in conjunction with bioassay measurements to generate an improved posterior probability distribution of the intake (Birchall A, 2007).

Building upon the Bayesian analysis method, IMBA utilizes its companion module, the uncertainty analyzer (UA) to perform more complex Bayesian analysis needed for predicting posterior probability distribution for biokinetic model parameters. The UA uses a Monte Carlo sampling method termed the Weighted Likelihood Monte Carlo Sampling Method (WeLMoS) which relies on a weighted Latin Hypercube method to calculate the Bayesian posterior distributions of parameters and dose. The WeLMoS method works by first generating random samples from the prior distribution of biokinetic parameters using Monte Carlo sampling protocols. Subsequently, each vector is weighted according to its likelihood (i.e. the probability of the data given the vector of parameters and the intake) and orders them in an increasing order of χ^2 (Puncher & Birchall, A Monte carlo method for calculating Bayesian uncertainties in internal dosimetry, 2008). In essence, the parameters are weighted according to how well the sampled intake and parameters fit the data (Puncher & Birchall, The autocorrelation coefficient as a tool for assessing goodness of fit between bioassay predicitons and measurment data, 2008). The weighted values are then used to calculate posterior distributions of intake and model parameters.

The uncertainty analyzer, as used in this project, is used in conjunction with IMBA-PPAE in order to implement the WeLMoS method. As a first step in the process, a sample matrix is constructed by the UA from a priori probability distribution defined by the user. The uncertainty analyzer then uses IMBA-PPAE to solve the pertinent biokinetic models in order to calculate intake and bioassay predictions over the required measurement times. This is accomplished by the uncertainty analyzer communicating directly with the critical subroutines contained in IMBA-PPAE, thus allowing for intake and dose calculations to be derived by Monte Carlo simulations. In the next stage of the process, the user specifies a range of discrete intakes or parameters that is assumed to contain the range of intake in the posterior distribution. Finally, intakes and bioassay predictions from the previous steps are used to calculate the weighted likelihood and posterior distributions for intake and model parameters (Puncher and Birchall 2008). The male and female cohorts are both tested by changing the same model parameters to better predict the intake.

4.6 IMBA Future Mode

The main objective of this study is to alter the default ^{90}Sr hermaphrodite model parameters to obtain an improved fit to the bioassay data, and improve the predictive capabilities of the calculated intake and long term skeletal retention. To accomplish this task, IMBA-PPAE provides a programming environment called future mode, in which customized models can be designed and saved as source files to be investigated using the uncertainty analyzer add on program. Some radionuclides have pre-loaded future mode systemic biokinetic models based on the ICRP 60 series that allows the user to adjust inter-compartmental transfer rates with the uncertainty analyzer program. However, IMBA-PPAE future mode did not contain a pre-exiting model in the case of ICRP 78 ^{90}Sr hermaphrodite model.

A custom model was created in IMBA-PPAE future mode to incorporate the transfer rates and kinetics of strontium in the body. The model shown in Figure 4.1 was implemented into IMBA future mode biokinetics tab Figure 4.2 with transfer rates as shown in Table 4.1. The developed model assumes that all of the internalized radionuclide enters directly into the transfer compartment. Once the radionuclide is the transfer compartment, it follows the biokinetic model through the body.

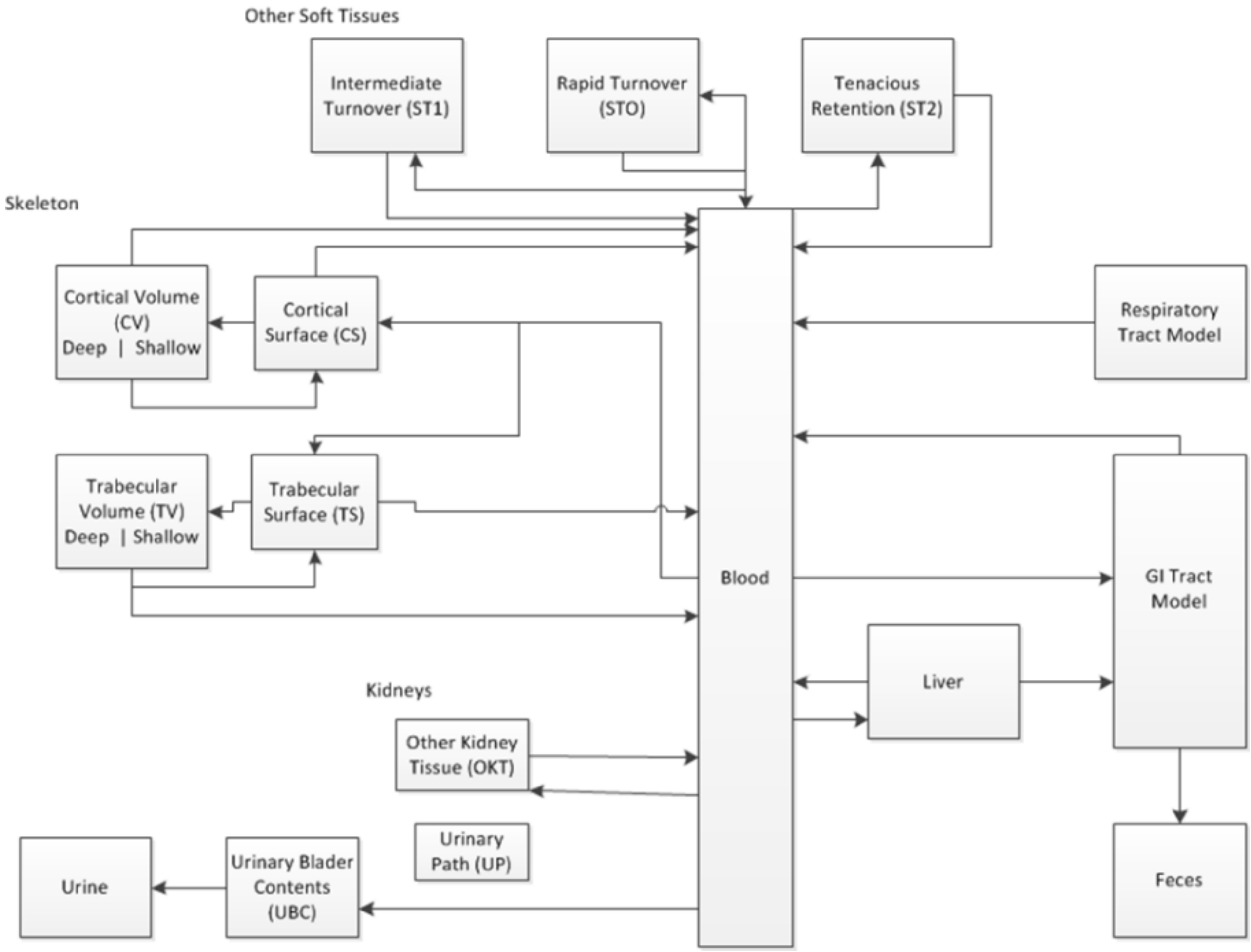

Figure 4.1: ICRP Default Model

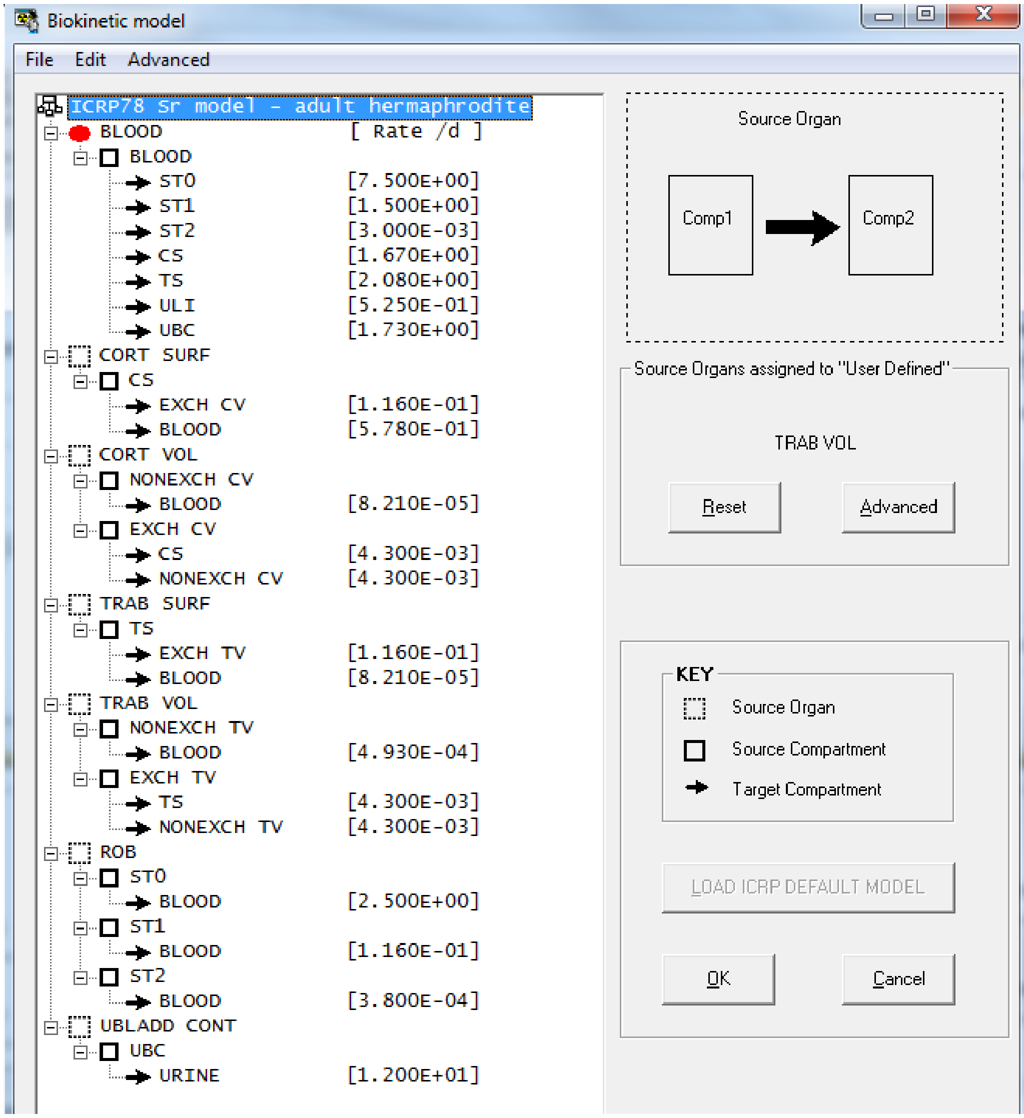

Figure 4.2 IMBA Future Mode Screen Shot

Table 4.1 ICRP 78 ^{90}Sr Default Transfer Parameters

Starting Compartment	Ending Compartment	Default Transfer Rate (d^{-1})
BLOOD	ST0	7.50E
BLOOD	ST1	1.50E
BLOOD	ST2	$3.00\ 10^{-3}$
BLOOD	CORTICAL SURFACE	1.67
BLOOD	TRABECULAR SURFACE	2.08
BLOOD	RC CONTENTS	$1.16\ 10^{-1}$
BLOOD	URIN BLADDER CONT	$5.78\ 10^{-1}$
CORTICAL SURFACE	EXCH CORT VOL	$1.16\ 10^{-1}$
CORTICAL SURFACE	BLOOD	$5.78\ 10^{-1}$
NONEX CORT VOL	BLOOD	$8.21\ 10^{-5}$
EXCH CORT VOL	CORTICAL SURFACE	$4.30\ 10^{-3}$
EXCH CORT VOL	NONEX CORT VOL	$4.30\ 10^{-3}$
TRABECULAR SURF	EXCH TRAB VOL	$1.16\ 10^{-1}$
TRABECULAR SURF	BLOOD	$8.21\ 10^{-4}$
NONEX TRAB VOL	BLOOD	$4.93\ 10^{-4}$
EXCH TRAB VOL	TRABECULAR SURFACE	$4.30\ 10^{-3}$
EXCH TRAB VOL	NONEXCH TRAB VOL	$4.30\ 10^{-3}$
ST0	BLOOD	2.50
ST1	BLOOD	$1.16\ 10^{-1}$
ST2	BLOOD	$3.80\ 10^{-4}$
URIN BLADDER CONT	URINE	12.0

4.7 Sensitivity Analysis

When evaluating the ^{90}Sr hermaphrodite model created in IMBA-PPAE future mode using the uncertainty analyzer, an issue arises because the UA restricts the user to only vary nine model parameters at any one time. In reality, it is likely that the alteration of some model parameters is unnecessary due to their negligible effect on the transfer kinetics. So, selecting the model parameters that have the largest effect on the predicted bioassay data as well as the ones that have the most physiological significance is worthwhile. A sensitivity analysis also aids in identifying the physiological processes and pathways that are associated with the transfer rates that heavily influence the bioassay predictions (Luciani A, 2001).

A sensitivity analysis of the model was conducted to establish which of the available parameters most influenced the modes predictive capability. Many methods have been proposed for evaluating sensitivity of model parameters in general applications (Hamby 1995). A differential sensitivity analysis was chose for this project, in part because of prior success shown in other biokinetic models (Luciani et. al. 2001).

In the differential method, the partial derivative of the mathematical expression is what describes the transfer kinetics between compartments in the model. The partial derivative of the dependent variable (excretion or retention rate) is calculated with respect to the independent variable, which is then used to calculate a sensitivity coefficient for the independent variable (Luciani A, 2001). The sensitivity coefficient (S_i) is defined as the ration of the relative exchange of the intake or retention rate (u) to the relative change of the respective model parameter (λ_i).

$$S_i = \frac{du}{d\lambda_i} * \frac{\lambda_i}{u} = \frac{\Delta u}{\Delta \lambda_i} * \frac{\lambda_i}{u} \qquad \textbf{(4.15)}$$

Equation 4.15 was modified to determine S_i using the default systemic model predicted values for activity retained in the whole blood, whole body, and skeleton to determine intake as follows:

$$S_i = \frac{\Delta I}{\Delta \lambda_i} * \frac{\lambda_i}{I} \qquad \textbf{(4.16)}$$

Where (I) is the intake predicted using the default parameter values for activity in whole blood, whole body, and skeleton at various times post-injection and (ΔI) is the change in the intake due to the change in the altered parameter ($\Delta\lambda_i$). Therefore, if a model's transfer rate is increased by 10% (i.e. $\Delta\lambda_i = 0.1*\lambda_i$), ($S_i$) can be expressed as follows:

$$S_i = 10 * \frac{\Delta I}{\mathrm{I}} \qquad \textbf{(4.17)}$$

A change of 10% was chosen as a convenient value to use in the sensitivity analysis since the effect of intake due to the change in the transfer rate was not affected by small rounding errors (Luciani et al. 2001).

Since the parameters in the systemic model are not gender specific, the sensitivity analysis was conducted for the model only once to determine the models' sensitive parameters. The sensitivity (S_i) parameter for all parameters was calculated. The eight parameters with the highest absolute value of (S_i) were determined to be the most sensitive and were selected to be varied in the uncertainty analyzer. Only eight of the nine total parameters were selected because the ninth most sensitive parameter did not aid in completing a full loop through any pathway in the system nor did was it relevant to the bioassay data available. The parameters incomplete loop would lead to pooling in a compartment that are not being simultaneously optimized thus not resemble any bioassay data, so therefore was disregarded and only eight parameters modeled.

4.8 Biokinetic Hyper-modeling

To implement the WeLMoS Monte Carlo method, the IMBA-PPAE future mode customized hermaphrodite systemic model was loaded. Subsequently, the eight most sensitive parameters as determined from the sensitivity analysis were selected to be varied in the uncertainty analyzer. A log-uniform distribution was specified for each parameter modeled. The range of the sampling regime was 0.05 to 50 times the value of the default parameters as suggested in the IMBA software manual. As the predicted values of the intake became closer to the known intake, the model parameters were varied over a decreased range to reduce the overall chi-squared. The Latin hyper-cube method was selected as a random sampling method and was used to from an [n*N] sample matrix, where (N) is the desired number of iterations and (n) is the number of biokinetic parameters to be varied (Puncher Birchall 2008). The number of simulations (N) in this study was selected to be $5*10^4$ for each set of iterations.

4.9 Optimization of Intake and Skeletal Retention Prediction

After completion of WeLMoS sampling, (N) sets of varied parameters and their associated intake were calculated and ordered from smallest to largest value of the chi-square statistic. The relative difference between the predicted and known intake was calculated using Equation 4.18.

$$Relative\ Difference = \left|\frac{(Measured - Predicted)}{\left(\frac{Measured + Predicted}{2}\right)}\right| * 100\% \qquad \textbf{(4.18)}$$

The model parameters what predicted the intake within 5% and resulted in a chi-squared value in the lowest 1% were selected for further analysis. This set of optimized parameters was then analyzed using the uncertainty analyzer again. In the subsequent optimizations, the sampling range was reduced from 0.05 to 50 to 0.5 to 5 to generate a finer adjustment of the model parameters. The reduction of the sampling range allowed the chi-squared to be reduced to its minimum.

A practical decision rule was established that the best model parameters were not only those that predicted the intake within 5% but also reduced the skeleton within the least overall relative difference. The WeLMoS procedure was then repeated as previously described until the predicted intake was reduced to within 5% and the predicted activity in the skeleton was also reduced. The multiple iterations within the smaller Monte Carlo sampling range allowed the chi-squared to be reduced to its minimum in a smaller number of iterative

Chapter 5 RESULTS AND DISCUSSION

5.1 Comparison of Default Model Predictions for the Male and Female Composite Cohorts

Using the method of maximum likelihood in IMBA-PPAE, estimates of intake were calculated based upon bioassay data including: whole blood, whole body counts, and skeletal retention at sacrifice. The calculated value of intake was then compared to the 82 and 205.2 μCi ($3.03*10^6$ & $7.60*10^6$ Bq) for the female and male cohorts, respectively. The difference was calculated and is shown in Table 5.1.

Table 5.1 Comparison of Default Intake Predictions and Measured Values

Sex	Default Predicted Intake (Bq)	Measured Intake (Bq)	Predicted Activity / Measured Activity	Relative Difference
Male	$1.24\ 10^6$	$7.60E\ 10^6$	0.16	144%
Female	$1.09\ 10^5$	$3.03\ 10^6$	0.04	186%

The values of the whole blood, whole body counts and retention in skeleton were calculated by inputting the known intake into the IMBA-PPAE software. The software then calculated the values of activity at the same specified times as the measured values. The measured and predicted values of bioassay samples as well as their difference are shown in Tables 5.2 through 5.7 and represented graphically in Figure 5.1to 5.6 for whole blood, whole body counts, and skeleton respectively.

Table 5.2 Male Comparison Whole Blood Predictions with Measured Values

Analysis Time (Days)	Default Predicted Activity In Whole Blood (Bq)	Male Cohort Measured Activity In Whole Blood (Bq)	Predicted Activity / Measured Activity	Relative Difference
1.81 10^{3}	2.25 10^{2}	2.12 10^{1}	1.06 10^{1}	166%
2.04 10^{3}	2.11 10^{2}	1.62 10^{1}	1.30 10^{1}	171%
2.19 10^{3}	2.01 10^{2}	1.04 10^{1}	1.93 10^{1}	180%
2.33 10^{3}	1.93 10^{2}	4.49	4.30 10^{1}	191%
2.50 10^{3}	1.83 10^{2}	4.52	4.06 10^{1}	190%
2.62 10^{3}	1.77 10^{2}	5.59	3.16 10^{1}	188%
2.81 10^{3}	1.67 10^{2}	4.42	3.77 10^{1}	190%
2.94 10^{3}	1.60 10^{2}	4.05	3.96 10^{1}	190%
3.10 10^{3}	1.53 10^{2}	3.59	4.26 10^{1}	191%
3.29 10^{3}	1.42 10^{2}	3.96	3.65 10^{1}	189%
3.46 10^{3}	1.37 10^{2}	5.42	2.53 10^{1}	185%
3.64 10^{3}	1.30 10^{2}	4.33E	3.00 10^{1}	187%
3.80 10^{3}	1.24 10^{2}	2.87	4.32 10^{1}	191%
4.04 10^{3}	1.15 10^{2}	5.96	1.94 10^{1}	180%
4.24 10^{3}	1.09 10^{2}	1.98	5.50 10^{1}	193%
4.39 10^{3}	1.04 10^{2}	2.95	3.53 10^{1}	189%
4.55 10^{3}	9.92 10^{1}	3.52	2.82 10^{1}	186%
4.78 10^{3}	9.27 10^{1}	2.87	3.23 10^{1}	188%
4.97 10^{3}	8.77 10^{1}	1.11	7.90 10^{1}	195%
5.14 10^{3}	8.35 10^{1}	2.12	3.94 10^{1}	190%
5.34 10^{3}	7.87 10^{1}	1.40	5.62 10^{1}	193%
5.70 10^{3}	7.09 10^{1}	1.50	4.73 10^{1}	192%
5.86 10^{3}	6.76 10^{1}	9.19 10^{-1}	7.36 10^{1}	195%

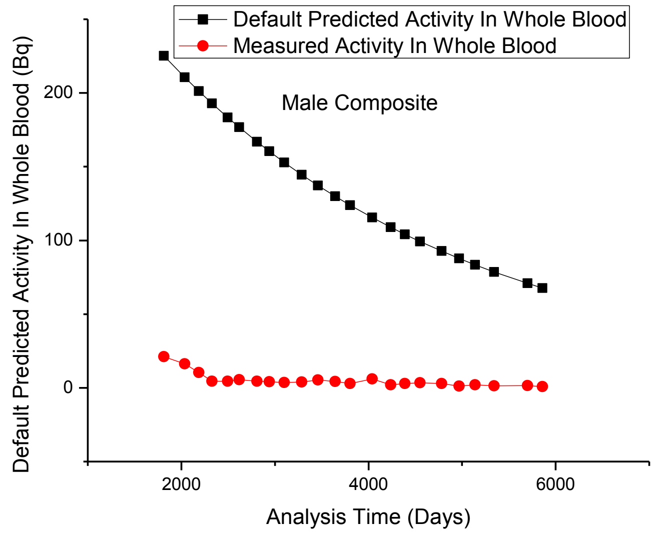

Figure 5.1 Male Comparison of Whole Blood Predictions with Measured Values

Table 5.3 Male Comparison Whole Body Count Predictions with Measured Values

Analysis Time (Days)	Default Predicted Activity In Whole Body Counts (Bq)	Male Cohort Measured Activity In Whole Body Counts (Bq)	Predicted Activity / Measured Activity	Relative Difference
$3.70\ 10^{1}$	$4.76\ 10^{6}$	$2.20\ 10^{6}$	2.16	74%
$8.50\ 10^{1}$	$4.68\ 10^{6}$	$1.89\ 10^{6}$	2.48E	85%
$3.59\ 10^{2}$	$4.47\ 10^{6}$	$1.41\ 10^{6}$	3.17	104%
$4.07\ 10^{2}$	$4.43\ 10^{6}$	$1.23\ 10^{6}$	3.60	113%
$5.22\ 10^{2}$	$4.34\ 10^{6}$	$1.03\ 10^{6}$	4.21	123%
$7.27\ 10^{2}$	$4.17\ 10^{6}$	$9.27\ 10^{5}$	4.50	127%
$7.97\ 10^{2}$	$4.12\ 10^{6}$	$8.74\ 10^{5}$	4.71	130%
$8.25\ 10^{2}$	$4.10\ 10^{6}$	$8.89\ 10^{5}$	4.61	129%
$1.02\ 10^{3}$	$3.95\ 10^{6}$	$7.37\ 10^{5}$	5.36	137%
$1.20\ 10^{3}$	$3.81\ 10^{6}$	$6.18\ 10^{5}$	6.17	144%
$1.46\ 10^{3}$	$3.64\ 10^{6}$	$5.61\ 10^{5}$	6.49	147%
$1.66\ 10^{3}$	$3.51\ 10^{6}$	$4.88\ 10^{5}$	7.19	151%
$1.81\ 10^{3}$	$3.41\ 10^{6}$	$4.57\ 10^{5}$	7.46	153%
$1.92\ 10^{3}$	$3.35\ 10^{6}$	$4.28\ 10^{5}$	7.82	155%
$2.24\ 10^{3}$	$3.16\ 10^{6}$	$3.79\ 10^{5}$	8.35	157%
$2.46\ 10^{3}$	$3.05\ 10^{6}$	$3.41\ 10^{5}$	8.94	160%
$2.66\ 10^{3}$	$2.94\ 10^{6}$	$3.38\ 10^{5}$	8.71	159%
$2.90\ 10^{3}$	$2.83\ 10^{6}$	$3.17\ 10^{5}$	8.93	160%
$3.09\ 10^{3}$	$2.74\ 10^{6}$	$3.05\ 10^{5}$	9.00	160%
$3.26\ 10^{3}$	$2.67\ 10^{6}$	$2.87\ 10^{5}$	9.31	161%
$3.58\ 10^{3}$	$2.54\ 10^{6}$	$2.81\ 10^{5}$	9.03	160%
$4.10\ 10^{3}$	$2.35\ 10^{6}$	$2.58\ 10^{5}$	9.09	160%
$4.53\ 10^{3}$	$2.20\ 10^{6}$	$2.28\ 10^{5}$	9.67	162%
$4.89\ 10^{3}$	$2.09\ 10^{6}$	$2.01\ 10^{5}$	10.4	165%
$5.27\ 10^{3}$	$1.99\ 10^{6}$	$2.05\ 10^{5}$	9.69	163%
$5.86\ 10^{3}$	$1.84\ 10^{6}$	$1.99\ 10^{5}$	9.23	161%

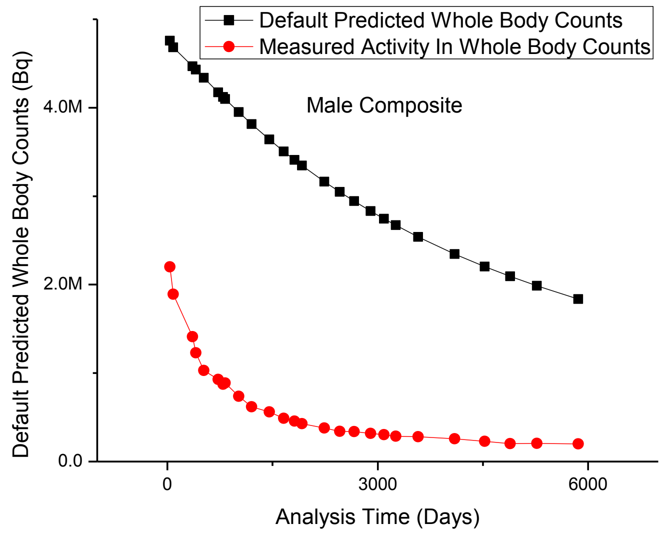

Figure 5.2 Male Comparison of Whole Body Count Predictions with Measured Values

Table 5.4 Male Comparison Skeletal Predictions with Measured Values

		Male Cohort		
Analysis Time (Days)	Default Predicted Activity In Skeleton (Bq)	Measured Activity In Skeleton (Bq)	Predicted Activity / Measured Activity	Relative Difference
$7.28\ 10^{2}$	$3.23\ 10^{6}$	$8.05\ 10^{5}$	4.02	120%
$7.40\ 10^{2}$	$3.22\ 10^{6}$	$7.44\ 10^{5}$	4.33	125%
$1.74\ 10^{3}$	$2.44\ 10^{6}$	$6.09\ 10^{5}$	4.00	120%
$2.31\ 10^{3}$	$2.08\ 10^{6}$	$2.73\ 10^{5}$	7.62	154%
$2.84\ 10^{3}$	$1.81\ 10^{6}$	$1.68\ 10^{5}$	10.8	166%
$4.60\ 10^{3}$	$1.13\ 10^{6}$	$4.36\ 10^{5}$	2.59	89%
$5.23\ 10^{3}$	$9.61\ 10^{5}$	$2.46\ 10^{5}$	3.91	118%
$5.86\ 10^{3}$	$8.20\ 10^{5}$	$1.94\ 10^{5}$	4.23	124%

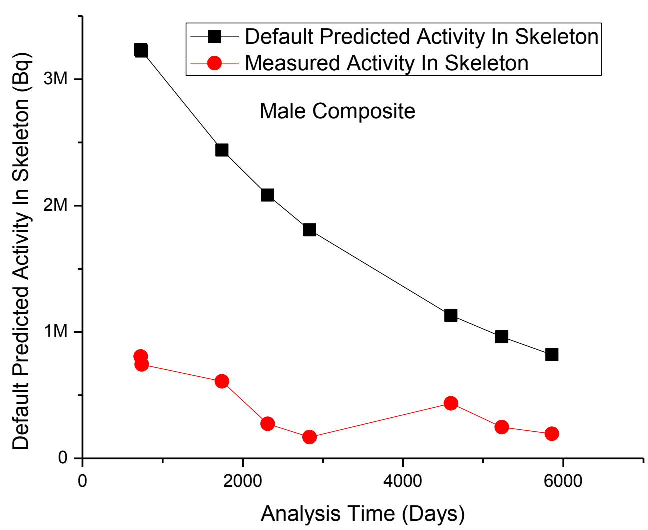

Figure 5.3 Male Comparison of Skeletal Predictions with Measured Values

Table 5.5 Female Comparison Whole Blood Predictions with Measured Values

Analysis Time (Days)	Default Predicted Activity In Whole Blood (Bq)	Female Cohort Measured Activity In Whole Blood (Bq)	Predicted Activity / Measured Activity	Relative Difference
1.82E 10^{3}	8.99 10^{1}	1.51 10^{1}	5.96	143%
2.04 10^{3}	8.41 10^{1}	9.40	8.94	160%
2.19 10^{3}	8.04 10^{1}	5.23	1.54 10^{1}	176%
2.33 10^{3}	7.71 10^{1}	2.59	2.98 10^{1}	187%
2.50 10^{3}	7.31 10^{1}	4.16	1.76 10^{1}	178%
2.62 10^{3}	7.05 10^{1}	2.68	2.63 10^{1}	185%
2.81 10^{3}	6.66 10^{1}	3.81	1.75 10^{1}	178%
2.94 10^{3}	6.41 10^{1}	2.98	2.15 10^{1}	182%
3.10 10^{3}	6.11 10^{1}	3.10	1.97 10^{1}	181%
3.29 10^{3}	5.78 10^{1}	3.22	1.79 10^{1}	179%
3.46 10^{3}	5.48 10^{1}	2.33	2.36 10^{1}	184%
3.64 10^{3}	5.19 10^{1}	2.49	2.08 10^{1}	182%
3.80 10^{3}	4.95 10^{1}	3.20	1.55 10^{1}	176%
4.05 10^{3}	4.60 10^{1}	2.29	2.01 10^{1}	181%
4.23 10^{3}	4.36 10^{1}	1.17	3.71 10^{1}	190%
4.39 10^{3}	4.16 10^{1}	3.46	1.20 10^{1}	169%
4.55 10^{3}	3.96 10^{1}	1.91	2.07 10^{1}	182%
4.78 10^{3}	3.70 10^{1}	5.07 10^{-1}	7.30 10^{1}	195%
4.97 10^{3}	3.50 10^{1}	1.23	2.85 10^{1}	186%
5.14 10^{3}	3.33 10^{1}	7.69 10^{-1}	4.34 10^{1}	191%
5.34 10^{3}	3.14 10^{1}	9.11 10^{-1}	3.45 10^{1}	189%
5.51 10^{3}	3.00 10^{1}	1.31	2.29 10^{1}	183%
5.70 10^{3}	2.83 10^{1}	8.42 10^{-1}	3.36 10^{1}	188%
5.85 10^{3}	2.71 10^{1}	5.33 10^{-1}	5.09 10^{1}	192%

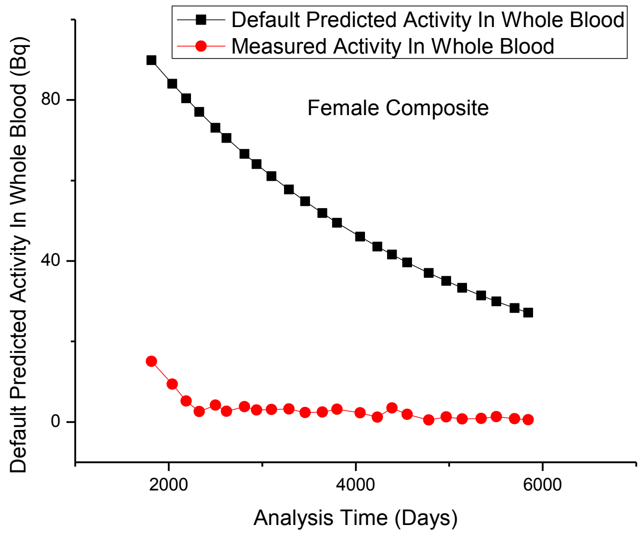

Figure 5.4 Female Comparison of Whole Blood Predictions with Measured Values

Table 5.6 Female Comparison Whole Body Count Predictions with Measured Values

Analysis Time (Days)	Default Predicted Activity In Whole Body Counts (Bq)	Female Cohort Measured Activity In Whole Body Counts (Bq)	Predicted Activity / Measured Activity	Relative Difference
$3.80\ 10^{1}$	$1.90\ 10^{6}$	$1.02\ 10^{6}$	1.86	60%
$4.20\ 10^{1}$	$1.89\ 10^{6}$	$1.64\ 10^{6}$	1.15	14%
$8.70\ 10^{1}$	$1.87\ 10^{6}$	$1.15\ 10^{6}$	1.63	48%
$1.33\ 10^{1}$	$1.85\ 10^{6}$	$9.10\ 10^{5}$	2.04	68%
$3.60\ 10^{2}$	$1.78\ 10^{6}$	$8.27\ 10^{5}$	2.16	73%
$4.08\ 10^{2}$	$1.77\ 10^{6}$	$7.27\ 10^{5}$	2.43	84%
$5.20\ 10^{2}$	$1.73\ 10^{6}$	$6.80\ 10^{5}$	2.55	87%
$7.96\ 10^{2}$	$1.65\ 10^{6}$	$4.72\ 10^{5}$	3.49	111%
$1.02\ 10^{3}$	$1.58\ 10^{6}$	$4.58\ 10^{5}$	3.44	110%
$1.20\ 10^{3}$	$1.52\ 10^{6}$	$4.10\ 10^{5}$	3.71	115%
$1.45\ 10^{3}$	$1.46\ 10^{6}$	$5.24\ 10^{5}$	2.78	94%
$1.66\ 10^{3}$	$1.40\ 10^{6}$	$3.21\ 10^{5}$	4.36	125%
$1.82\ 10^{3}$	$1.36\ 10^{6}$	$1.82\ 10^{5}$	7.49	153%
$2.26\ 10^{3}$	$1.26\ 10^{6}$	$2.26\ 10^{5}$	5.58	139%
$2.47\ 10^{3}$	$1.21\ 10^{6}$	$2.14\ 10^{5}$	5.67	140%
$2.66\ 10^{3}$	$1.18\ 10^{6}$	$1.99\ 10^{5}$	5.91	142%
$2.89\ 10^{3}$	$1.13\ 10^{6}$	$1.96\ 10^{5}$	5.78	141%
$3.13\ 10^{3}$	$1.09\ 10^{6}$	$1.80\ 10^{5}$	6.05	143%
$3.43\ 10^{3}$	$1.04\ 10^{6}$	$1.77\ 10^{5}$	5.86	142%
$3.76\ 10^{3}$	$9.87\ 10^{5}$	$1.52\ 10^{5}$	6.48	147%
$4.02\ 10^{3}$	$9.48\ 10^{5}$	$1.44\ 10^{5}$	6.58	147%
$4.68\ 10^{3}$	$8.61\ 10^{5}$	$1.62\ 10^{5}$	5.31	137%
$5.27\ 10^{3}$	$7.93\ 10^{5}$	$1.54\ 10^{5}$	5.16	135%
$5.85\ 10^{3}$	$7.35\ 10^{5}$	$1.40\ 10^{5}$	5.25	136%

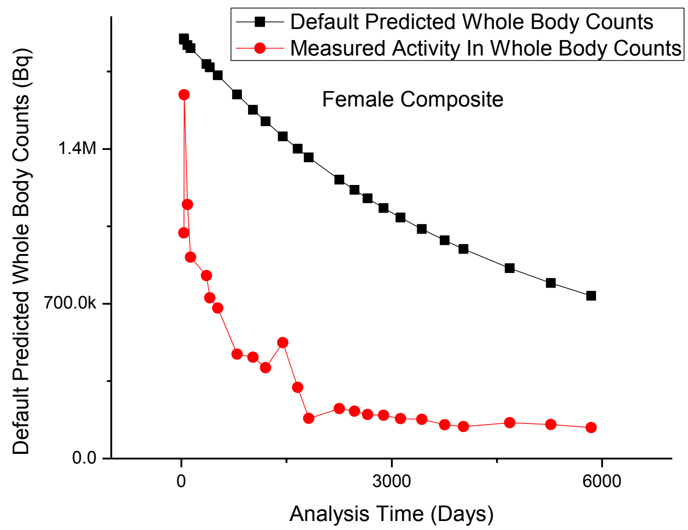

Figure 5.5 Female Comparison of Whole Body Count Predictions with Measured Values

Table 5.7 Female Comparison Skeletal Predictions with Measured Values

		Female Cohort		
Analysis Time (Days)	Default Predicted Activity In Skeleton (Bq)	Measured Activity In Skeleton (Bq)	Predicted Activity / Measured Activity	Relative Difference
$1.33\ 10^{2}$	$1.50\ 10^{6}$	$8.89\ 10^{5}$	1.69	51%
$1.42\ 10^{3}$	$1.07\ 10^{6}$	$4.31\ 10^{5}$	2.47	85%
$1.69\ 10^{3}$	$9.88\ 10^{5}$	$4.82\ 10^{5}$	2.05	69%
$1.80\ 10^{3}$	$9.59\ 10^{5}$	$1.51\ 10^{5}$	6.33	145%
$1.81\ 10^{3}$	$9.56\ 10^{5}$	$1.50\ 10^{5}$	6.35	146%
$1.82\ 10^{3}$	$9.53\ 10^{5}$	$1.12\ 10^{5}$	8.51	158%
$1.82\ 10^{3}$	$9.52\ 10^{5}$	$3.25\ 10^{5}$	2.93	98%
$2.81\ 10^{3}$	$7.26\ 10^{5}$	$1.95\ 10^{5}$	3.73	115%
$3.93\ 10^{3}$	$5.39\ 10^{5}$	$1.02\ 10^{5}$	5.27	136%
$5.85\ 10^{3}$	$3.29\ 10^{5}$	$1.29\ 10^{5}$	2.55	87%

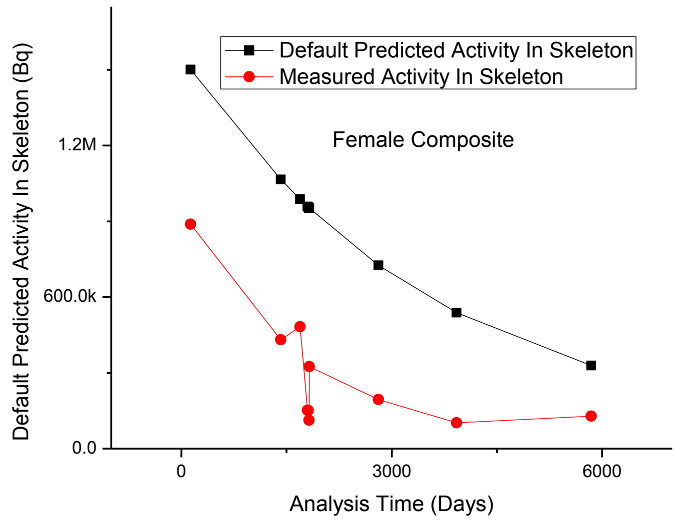

Figure 5.6 Female Comparison of Skeletal Predictions with Measured Values

5.2 Modification of Default Parameters

The eight most influential parameters as determined for the male and female cohorts were selected for modification with the IMBA-PPAE add on program the uncertainty program as previously described. The eight most influential parameters were first optimized for the predicted intake. To improve the value of the predicted intake the parameters were varied over a range of 0.05 to 50 times the default model parameters. The set of parameters that predicted the intake within 5% and in the lowest 1% of the chi-squared value were selected for further iterations. Further iterations in a smaller range of values allowed for the ability to fine tune the model parameters and reduce the overall chi-squared for the skeleton. A comparison of the default model as well as the optimized model for the male and female cohorts can be seen in Table 5.8. Evaluating the optimized model parameters intake predictive capabilities improve as well as the predicted bioassay measurements as shown in Table 5.9 to 5.16 and illustrated in Figure 5.7 to 5.13.

Table 5.8 Model Parameters Default and Modified

Starting Compartment	Ending Compartment	Default Transfer Rate	Male Modified Transfer Rate	Female Modified Transfer Rate
BLOOD	ST0	7.50	7.50	7.50
BLOOD	ST1	1.50	1.50	1.50
BLOOD	ST2	$3.00\ 10^{-3}$	$3.00\ 10^{-3}$	$3.00\ 10^{-3}$
BLOOD	CORTICAL SURFACE	1.67	11.67	1.67
BLOOD	TRABECULAR SURFACE	2.08	2.08	2.08
BLOOD	**RC CONTENTS**	**$1.16\ 10^{-1}$**	**$1.52\ 10^{-1}$**	**$1.26\ 10^{-4}$**
BLOOD	**URIN BLADDER CONT**	**$5.78\ 10^{-1}$**	**7.56**	**3.96**
CORTICAL SURFACE	**EXCH CORT VOL**	**$1.16\ 10^{-1}$**	**1.01**	**$1.01\ 10^{-1}$**
CORTICAL SURFACE	BLOOD	$5.78\ 10^{-1}$	$5.78\ 10^{-1}$	$5.78\ 10^{-1}$
NONEX CORT VOL	**BLOOD**	**$8.21\ 10^{-5}$**	**$4.65\ 10^{-4}$**	**$7.69\ 10^{-7}$**
EXCH CORT VOL	CORTICAL SURFACE	$4.30\ 10^{-3}$	$4.30\ 10^{-3}$	$4.30\ 10^{-3}$
EXCH CORT VOL	**NONEX CORT VOL**	**$4.30\ 10^{-3}$**	**$4.19\ 10^{-2}$**	**1.94**
TRABECULAR SURF	**EXCH TRAB VOL**	**$1.16\ 10^{-1}$**	**$1.61\ 10^{-1}$**	**$7.61\ 10^{-2}$**
TRABECULAR SURF	BLOOD	$8.21\ 10^{-4}$	$8.21\ 10^{-4}$	$8.21\ 10^{-4}$
NONEX TRAB VOL	**BLOOD**	**$4.93\ 10^{-4}$**	**$6.73\ 10^{-3}$**	**2.69**
EXCH TRAB VOL	TRABECULAR SURFACE	$4.30\ 10^{-3}$	$4.30\ 10^{-3}$	$4.30\ 10^{-3}$
EXCH TRAB VOL	**NONEXCH TRAB VOL**	**$4.30\ 10^{-3}$**	**$3.74\ 10^{-2}$**	**6.99**
ST0	BLOOD	2.50	2.50	2.50
ST1	BLOOD	$1.16\ 10^{-1}$	$1.16\ 10^{-1}$	$1.16\ 10^{-1}$
ST2	BLOOD	$3.80\ 10^{-4}$	$3.80\ 10^{-4}$	$3.80\ 10^{-4}$
URIN BLAD CONT	URINE	12.0	12.0	12.0

Table 5.9 Comparison of Optimized Intake Predictions

Sex	Modified Predicted Intake (Bq)	Measured Intake (Bq)	Predicted Activity / Measured Activity	Relative Difference
Male	$7.71\ 10^{6}$	$7.60\ 10^{6}$	1.02	2%
Female	$3.08\ 10^{6}$	$3.03\ 10^{6}$	1.02	2%

Table 5.10 Modified Male Whole Blood Predictions

Analysis Time (Days)	Modified Predicted Activity In Whole Blood (Bq)	Male Cohort Measured Activity In Whole Blood (Bq)	Predicted Activity / Measured Activity	Relative Difference
$1.81\ 10^{3}$	$2.11\ 10^{1}$	$2.12\ 10^{1}$	$9.94\ 10^{-1}$	1%
$2.04\ 10^{3}$	$1.89\ 10^{1}$	$1.62\ 10^{1}$	1.17	15%
$2.19\ 10^{3}$	$1.76\ 10^{1}$	$1.04\ 10^{1}$	1.69	51%
$2.33\ 10^{3}$	$1.65\ 10^{1}$	4.49	3.67	114%
$2.50\ 10^{3}$	$1.52\ 10^{1}$	4.52	3.36	108%
$2.62\ 10^{3}$	$1.43\ 10^{1}$	5.59	2.56	88%
$2.81\ 10^{3}$	$1.31\ 10^{1}$	4.42	2.96	99%
$2.94\ 10^{3}$	$1.23\ 10^{1}$	4.05	3.04	101%
$3.10\ 10^{3}$	$1.14\ 10^{1}$	3.59	3.18	104%
$3.29\ 10^{3}$	$1.04\ 10^{1}$	3.96	2.64	90%
$3.46\ 10^{3}$	9.62	5.42	1.77	56%
$3.64\ 10^{3}$	8.81	4.33	2.04	68%
$3.80\ 10^{3}$	8.17	2.87	2.85	96%
$4.04\ 10^{3}$	7.30	5.96	1.23	20%
$4.24\ 10^{3}$	6.65	1.98	3.36	108%
$4.39\ 10^{3}$	6.19	2.95	2.10	71%
$4.55\ 10^{3}$	5.73	3.52	1.63	48%
$4.78\ 10^{3}$	5.14	2.87	1.79	57%
$4.97\ 10^{3}$	4.70	1.11	4.23	124%
$5.14\ 10^{3}$	4.34	2.12	2.05	69%
$5.34\ 10^{3}$	3.94	1.40	2.81	95%
$5.70\ 10^{3}$	3.32	1.50	2.22	76%
$5.86\ 10^{3}$	3.08	$9.19\ 10^{-1}$	3.35	108%

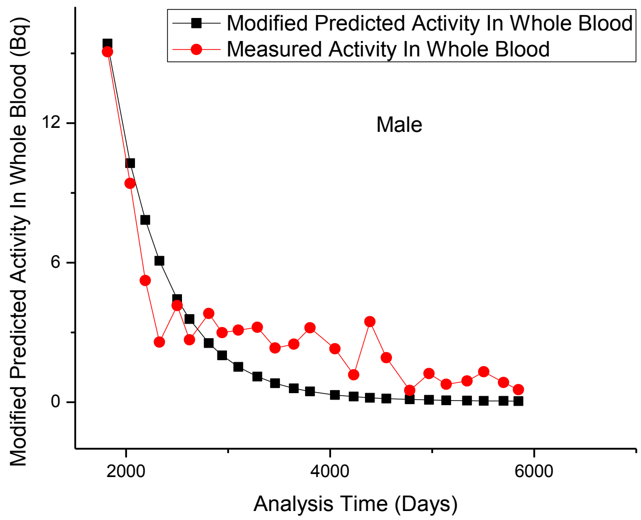

Figure 5.7 Modified Male Comparison of Whole Blood Predictions

Table 5.11 Modified Male Whole Body Count Predictions

Analysis Time (Days)	Modified Predicted Activity In Whole Body Counts (Bq)	Measured Activity In Whole Body Counts (Bq)	Predicted Activity / Measured Activity	Relative Difference
$3.70\ 10^{1}$	$2.23\ 10^{6}$	$2.20\ 10^{6}$	1.01	1%
$8.50\ 10^{1}$	$1.98\ 10^{6}$	$1.89\ 10^{6}$	1.05	4%
$3.59\ 10^{2}$	$1.15\ 10^{6}$	$1.41\ 10^{6}$	$8.15\ 10^{-1}$	20%
$4.07\ 10^{2}$	$1.08\ 10^{6}$	$1.23\ 10^{6}$	$8.78\ 10^{-1}$	13%
$5.22\ 10^{2}$	$9.59\ 10^{5}$	$1.03\ 10^{6}$	$9.31\ 10^{-1}$	7%
$7.27\ 10^{2}$	$8.26\ 10^{5}$	$9.27\ 10^{5}$	$8.91\ 10^{-1}$	11%
$7.97\ 10^{2}$	$7.94\ 10^{5}$	$8.74\ 10^{5}$	$9.09\ 10^{-1}$	10%
$8.25\ 10^{2}$	$7.83\ 10^{5}$	$8.89\ 10^{5}$	$8.80\ 10^{-1}$	13%
$1.02\ 10^{3}$	$7.14\ 10^{5}$	$7.37\ 10^{5}$	$9.69\ 10^{-1}$	3%
$1.20\ 10^{3}$	$6.60\ 10^{5}$	$6.18\ 10^{5}$	1.07	7%
$1.46\ 10^{3}$	$5.97\ 10^{5}$	$5.61\ 10^{5}$	1.06	6%
$1.66\ 10^{3}$	$5.52\ 10^{5}$	$4.88\ 10^{5}$	1.13	12%
$1.81\ 10^{3}$	$5.22\ 10^{5}$	$4.57\ 10^{5}$	1.14	13%
$1.92\ 10^{3}$	$5.02\ 10^{5}$	$4.28\ 10^{5}$	1.17	16%
$2.24\ 10^{3}$	$4.47\ 10^{5}$	$3.79\ 10^{5}$	1.18	16%
$2.46\ 10^{3}$	$4.14\ 10^{5}$	$3.41\ 10^{5}$	1.21	19%
$2.66\ 10^{3}$	$3.86\ 10^{5}$	$3.38\ 10^{5}$	1.14	13%
$2.90\ 10^{3}$	$3.56\ 10^{5}$	$3.17\ 10^{5}$	1.12	12%
$3.09\ 10^{3}$	$3.35\ 10^{5}$	$3.05\ 10^{5}$	1.10	9%
$3.26\ 10^{3}$	$3.17\ 10^{5}$	$2.87\ 10^{5}$	1.11	10%
$3.58\ 10^{3}$	$2.87\ 10^{5}$	$2.81\ 10^{5}$	1.02	2%
$4.10\ 10^{3}$	$2.46\ 10^{5}$	$2.58\ 10^{5}$	$9.55\ 10^{-1}$	5%
$4.53\ 10^{3}$	$2.19\ 10^{5}$	$2.28\ 10^{5}$	$9.61\ 10^{-1}$	4%
$4.89\ 10^{3}$	$2.00\ 10^{5}$	$2.01\ 10^{5}$	$9.93\ 10^{-1}$	1%
$5.27\ 10^{3}$	$1.82\ 10^{5}$	$2.05\ 10^{5}$	$8.87\ 10^{-1}$	12%
$5.86\ 10^{3}$	$1.60\ 10^{5}$	$1.99\ 10^{5}$	$8.02\ 10^{-1}$	22%

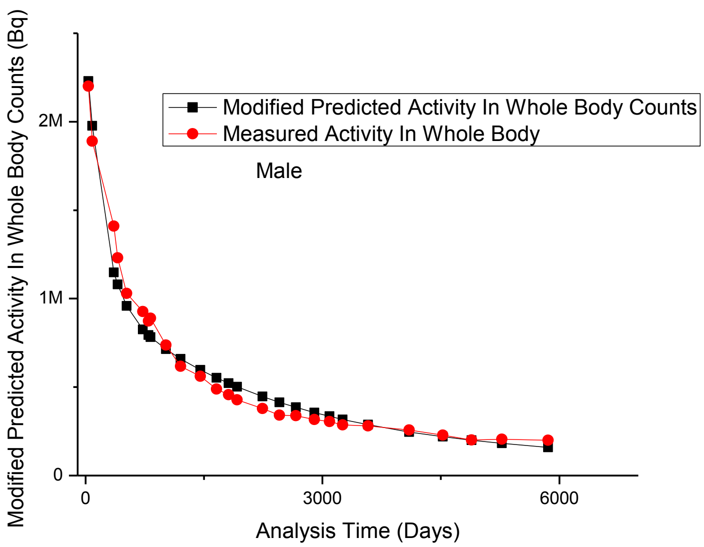

Figure 5.8 Modified Male Whole Body Count Predictions

Table 5.12 Modified Male Skeletal Predictions

	Male Cohort			
Analysis Time (Days)	Modified Predicted Activity In Skeleton (Bq)	Measured Activity In Skeleton (Bq)	Predicted Activity / Measured Activity	Relative Difference
$7.28\ 10^{2}$	$6.93\ 10^{5}$	$8.05\ 10^{5}$	$8.61\ 10^{-1}$	15%
$7.40\ 10^{2}$	$6.87\ 10^{5}$	$7.44\ 10^{5}$	$9.24\ 10^{-1}$	8%
$1.74\ 10^{3}$	$4.08\ 10^{5}$	$6.09\ 10^{5}$	$6.70\ 10^{-1}$	40%
$2.31\ 10^{3}$	$3.11\ 10^{5}$	$2.73\ 10^{5}$	1.14	13%
$2.84\ 10^{3}$	$2.43\ 10^{5}$	$1.68\ 10^{5}$	1.45	37%
$4.60\ 10^{3}$	$1.05\ 10^{5}$	$4.36\ 10^{5}$	$2.41\ 10^{-1}$	122%
$5.23\ 10^{3}$	$7.79\ 10^{4}$	$2.46\ 10^{5}$	$3.16\ 10^{-1}$	104%
$5.86\ 10^{3}$	$5.78\ 10^{4}$	$1.94\ 10^{5}$	$2.98\ 10^{-1}$	108%

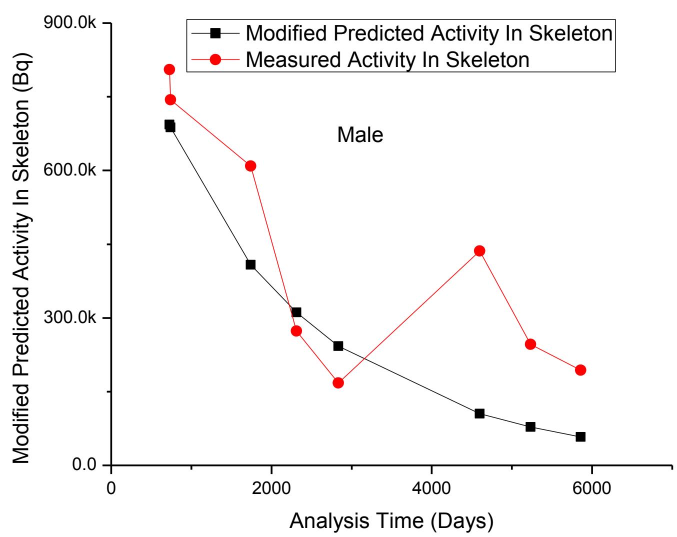

Figure 5.9 Modified Male Skeletal Predictions

Table 5.13 Modified Female Whole Blood Predictions

Analysis Time (Days)	Modified Predicted Activity In Whole Blood (Bq)	Female Cohort Measured Activity In Whole Blood (Bq)	Predicted Activity / Measured Activity	Relative Difference
$1.82\ 10^{3}$	1.54E+01	$1.51\ 10^{1}$	1.02	2%
$2.04\ 10^{3}$	1.03E+01	9.40	1.09	9%
$2.19\ 10^{3}$	7.84E+00	5.23	1.50	40%
$2.33\ 10^{3}$	6.08E+00	2.59	2.35	81%
$2.50\ 10^{3}$	4.43E+00	4.16	1.07	6%
$2.62\ 10^{3}$	3.57E+00	2.68	1.33	28%
$2.81\ 10^{3}$	2.54E+00	3.81	$6.65\ 10^{-1}$	40%
$2.94\ 10^{3}$	2.01E+00	2.98	$6.75\ 10^{-1}$	39%
$3.10\ 10^{3}$	1.52E+00	3.10	$4.91\ 10^{-1}$	68%
$3.29\ 10^{3}$	1.10E+00	3.22	$3.40\ 10^{-1}$	99%
$3.46\ 10^{3}$	8.14E-01	2.33	$3.50\ 10^{-1}$	96%
$3.64\ 10^{3}$	5.97E-01	2.49	$2.40\ 10^{-1}$	123%
$3.80\ 10^{3}$	4.60E-01	3.20	$1.44\ 10^{-1}$	150%
$4.05\ 10^{3}$	3.13E-01	2.29	$1.36\ 10^{-1}$	152%
$4.23\ 10^{3}$	2.38E-01	1.17	$2.02\ 10^{-1}$	133%
$4.39\ 10^{3}$	1.90E-01	3.46	$5.50\ 10^{-2}$	179%
$4.55\ 10^{3}$	1.53E-01	1.91	$8.01\ 10^{-2}$	170%
$4.78\ 10^{3}$	1.16E-01	$5.07\ 10^{-1}$	$2.28\ 10^{-1}$	126%
$4.97\ 10^{3}$	9.43E-02	1.23	$7.67\ 10^{-2}$	172%
$5.14\ 10^{3}$	8.00E-02	$7.69\ 10^{-1}$	$1.04\ 10^{-1}$	162%
$5.34\ 10^{3}$	6.73E-02	$9.11\ 10^{-1}$	$7.39\ 10^{-2}$	172%
$5.51\ 10^{3}$	5.96E-02	1.31	$4.54\ 10^{-2}$	183%
$5.70\ 10^{3}$	5.25E-02	8.42E-01	$6.24\ 10^{-2}$	177%
$5.85\ 10^{3}$	4.83E-02	5.33E-01	$9.07\ 10^{-2}$	167%

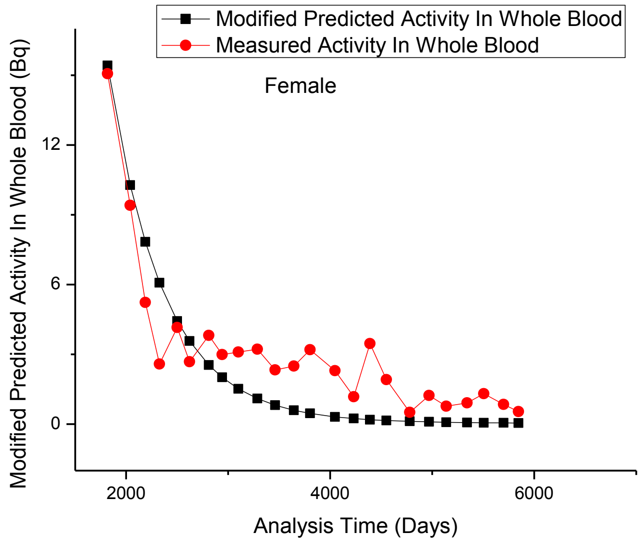

Figure 5.10 Modified Female Whole Blood Predictions

Table 5.14 Modified Female Whole Body Count

Analysis Time (Days)	Modified Predicted Activity In Whole Body Counts (Bq)	Female Cohort Measured Activity In Whole Body Counts (Bq)	Predicted Activity / Measured Activity	Relative Difference
$3.80\ 10^{1}$	$1.10\ 10^{6}$	$1.02\ 10^{6}$	1.08	7%
$4.20\ 10^{1}$	$1.09\ 10^{6}$	$1.64\ 10^{6}$	$6.62\ 10^{-1}$	41%
$8.70\ 10^{1}$	$1.01\ 10^{6}$	$1.15\ 10^{6}$	$8.79\ 10^{-1}$	13%
$1.33\ 10^{2}$	$9.41\ 10^{5}$	$9.10\ 10^{5}$	1.03	3%
$3.60\ 10^{2}$	$6.77\ 10^{5}$	$8.27\ 10^{5}$	$8.19\ 10^{-1}$	20%
$4.08\ 10^{2}$	$6.34\ 10^{5}$	$7.27\ 10^{5}$	$8.73\ 10^{-1}$	14%
$5.20\ 10^{2}$	$5.47\ 10^{5}$	$6.80\ 10^{5}$	$8.05\ 10^{-1}$	22%
$7.96\ 10^{2}$	$3.95\ 10^{5}$	$4.72\ 10^{5}$	$8.36\ 10^{-1}$	18%
$1.02\ 10^{3}$	$3.15\ 10^{5}$	$4.58\ 10^{5}$	$6.89\ 10^{-1}$	37%
$1.20\ 10^{3}$	$2.72\ 10^{5}$	$4.10\ 10^{5}$	$6.62\ 10^{-1}$	41%
$1.45\ 10^{3}$	$2.30\ 10^{5}$	$5.24\ 10^{5}$	$4.40\ 10^{-1}$	78%
$1.66\ 10^{3}$	$2.06\ 10^{5}$	$3.21\ 10^{5}$	$6.42\ 10^{-1}$	44%
$1.82\ 10^{3}$	$1.93\ 10^{5}$	$1.82\ 10^{5}$	1.06	6%
$2.26\ 10^{3}$	$1.69\ 10^{5}$	$2.26\ 10^{5}$	$7.51\ 10^{-1}$	29%
$2.47\ 10^{3}$	$1.62\ 10^{5}$	$2.14\ 10^{5}$	$7.58\ 10^{-1}$	28%
$2.66\ 10^{3}$	$1.57\ 10^{5}$	$1.99\ 10^{5}$	$7.90\ 10^{-1}$	23%
$2.89\ 10^{3}$	$1.53\ 10^{5}$	$1.96\ 10^{5}$	$7.79\ 10^{-1}$	25%
$3.13\ 10^{3}$	$1.49\ 10^{5}$	$1.80\ 10^{5}$	$8.25\ 10^{-1}$	19%
$3.43\ 10^{3}$	$1.44\ 10^{5}$	$1.77\ 10^{5}$	$8.14\ 10^{-1}$	21%
$3.76\ 10^{3}$	$1.40\ 10^{5}$	$1.52\ 10^{5}$	$9.22\ 10^{-1}$	8%
$4.02\ 10^{3}$	$1.38\ 10^{5}$	$1.44\ 10^{5}$	$9.54\ 10^{-1}$	5%
$4.68\ 10^{3}$	$1.31\ 10^{5}$	$1.62\ 10^{5}$	$8.10\ 10^{-1}$	21%
$5.27\ 10^{3}$	$1.26\ 10^{5}$	$1.54\ 10^{5}$	$8.19\ 10^{-1}$	20%
$5.85\ 10^{3}$	$1.21\ 10^{5}$	$1.40\ 10^{5}$	$8.65\ 10^{-1}$	14%

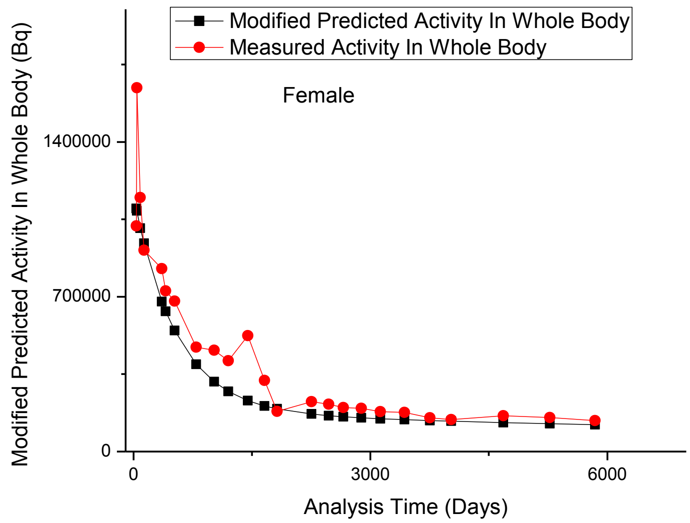

Figure 5.11 Modified Female Whole Body Count

Table 5.15 Modified Female Skeletal Predictions

Female Cohort				
Analysis Time (Days)	Modified Predicted Activity In Skeleton (Bq)	Measured Activity In Skeleton (Bq)	Predicted Activity / Measured Activity	Relative Difference
$1.33\ 10^{2}$	$9.34\ 10^{5}$	$8.89\ 10^{5}$	1.05	5%
$1.42\ 10^{3}$	$2.33\ 10^{5}$	$4.31\ 10^{5}$	$5.40\ 10^{-1}$	60%
$1.69\ 10^{3}$	$2.02\ 10^{5}$	$4.82\ 10^{5}$	$4.18\ 10^{-1}$	82%
$1.80\ 10^{3}$	$1.93\ 10^{5}$	$1.51\ 10^{5}$	1.27	24%
$1.81\ 10^{3}$	$1.92\ 10^{5}$	$1.50\ 10^{5}$	1.28	24%
$1.82\ 10^{3}$	$1.91\ 10^{5}$	$1.12\ 10^{5}$	1.71	52%
$1.82\ 10^{3}$	$1.91\ 10^{5}$	$3.25\ 10^{5}$	$5.89\ 10^{-1}$	52%
$2.81\ 10^{3}$	$1.53\ 10^{5}$	$1.95\ 10^{5}$	$7.87\ 10^{-1}$	24%
$3.93\ 10^{3}$	$1.38\ 10^{5}$	$1.02\ 10^{5}$	1.35	30%
$5.85\ 10^{3}$	$1.21\ 10^{5}$	$1.29\ 10^{5}$	$9.39\ 10^{-1}$	6%

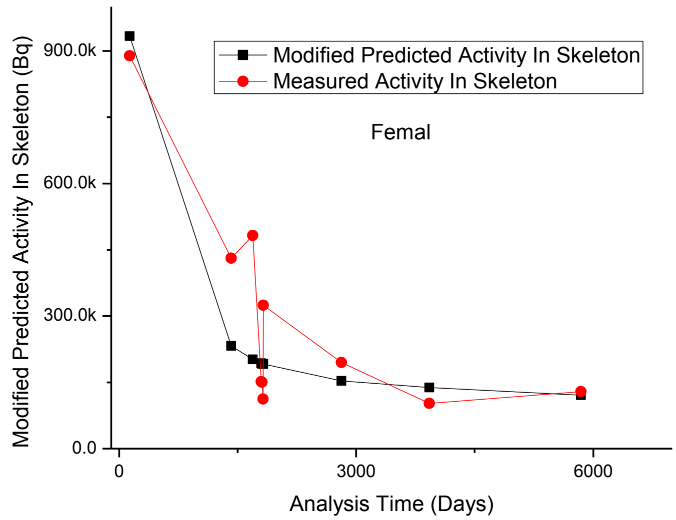

Figure 5.12 Modified Female Skeletal Predictions

Evaluating the retention in skeleton for both the male and female cohorts did not represent a perfect match for each data point, but represented the data set much better than when comparing the difference of the modified parameters and the default parameter predictions. The major issue arises in the female skeletal data set for the points around 1,500 days post injection. The suspected reasoning for this discrepancy is that the two monkeys in question gave birth, thus decreasing the activity retained in their skeleton. A potential remedy for this would be to add in the skeletal data of their offspring to the value of their mothers and see how they compare. While this was not the purpose of the study, it is evident that it has a large effect on the data set and is currently being investigated further by another graduate student. To visually evaluate the improvement in the predictive capability of the model, the whole body counts and activity in skeleton for both the female and male were plotted Figure 5.7 to 5.10. It can be shown that the agreement between the improved model fit and the data is better than that of the default model.

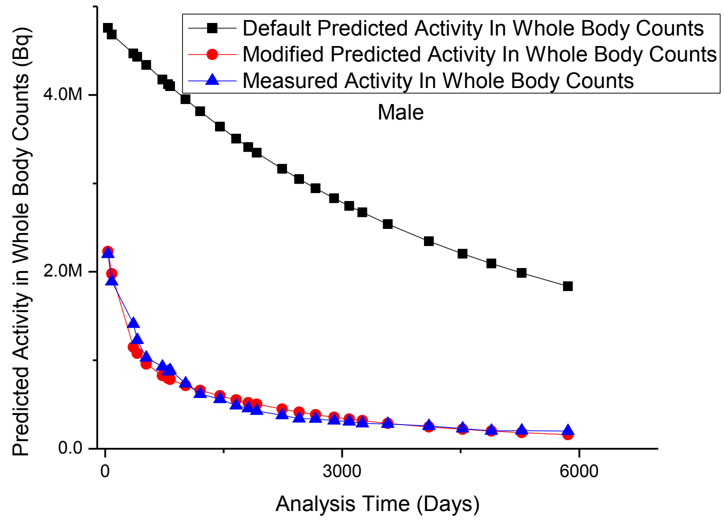

Figure 5.13 Default vs. Modified Model in Male Whole Body Counts

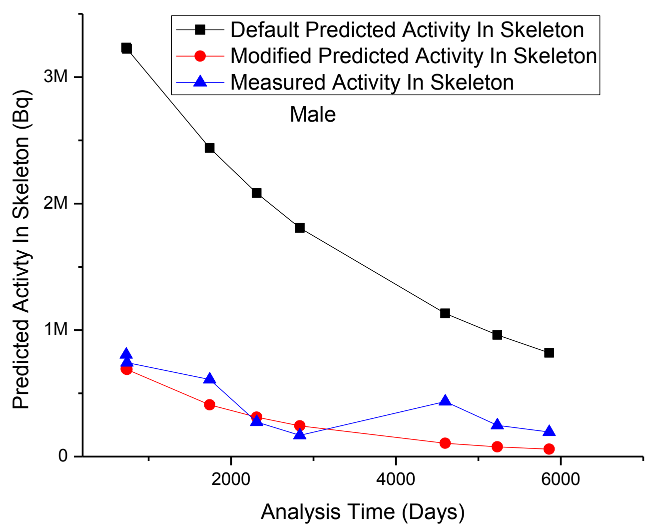

Figure 5.14 Default vs. Modified Model in Male Skeleton

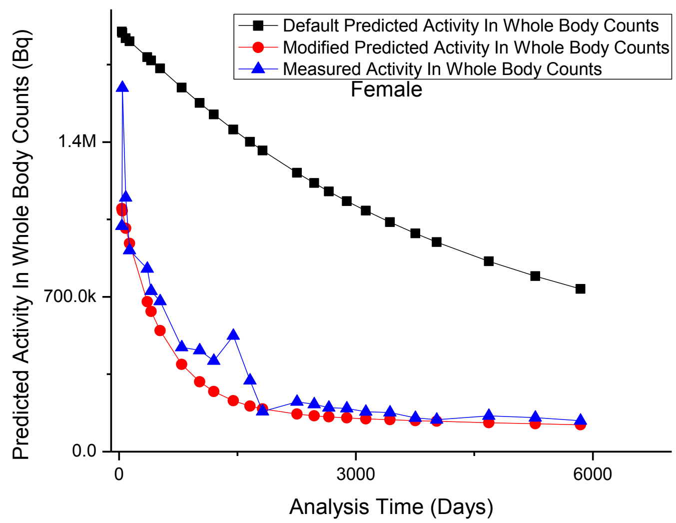

Figure 5.15 Default vs. Modified Model in Female Whole Body Counts

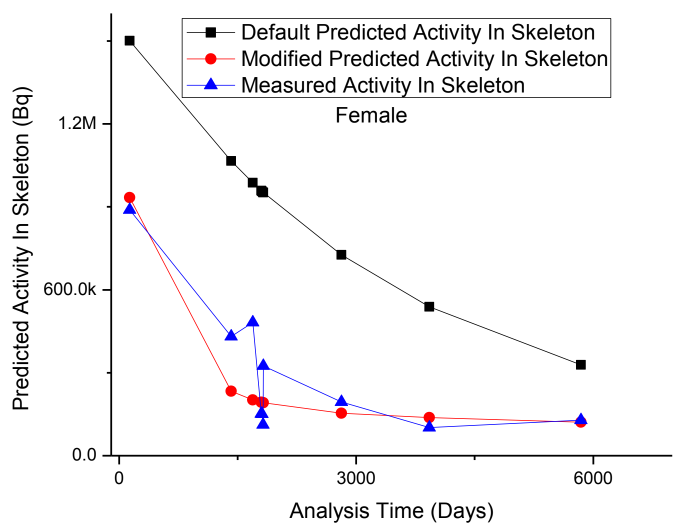

Figure 5.16 Default vs. Modified Model in Female Skeleton

Chapter 6 OPTIMIZED MODEL VALIDAITON

6.1 Independent Evaluation of Optimized Parameters

To validate a models predictive capabilities independent quality control checks are necessary. To achieve independent verification of an improved human model, non-human primate data not used in the generation of the models were reserved for evaluation. Four male cases and six female cases were used to independently evaluate the model. The cases tested had different characteristics than that of the ones used to develop the mode, including different times to sacrifice post injection and types of injection: intravenous, inter-paretenial, and inter-muscular. The multiple types of injection were evaluated to determine if the overall model has been improved.

The optimized model was evaluated by inputting the measured whole blood, whole body counts and skeletal data into IMBA-PPAE and independently calculated. The calculated intake of the individual cases was subsequently compared to the known values Table 6.1 to 6.2 and the relative difference shown in Figure 6.1-6.2 for the male and female cohorts respectively.

Table 6.1 Independent Predicted Intake Comparison in Male Subjects

Predicted Male Intake						
	Time Post Injection	Injected Activity (Measured)	IMBA Calculated (Default)	IMBA Calculated (Modified)	IMBA Calculated (Default) Comparison	IMBA Calculated (Modified) Comparison
R313M	150	$1.65\ 10^{6}$	$1.24\ 10^{6}$	$2.40\ 10^{6}$	28.6%	36.9%
R310M	67	$3.31\ 10^{6}$	$3.51\ 10^{6}$	$5.28\ 10^{6}$	5.8%	45.9%
R62M	5853	$6.23\ 10^{6}$	$3.10\ 10^{5}$	$3.06\ 10^{6}$	181.0%	68.2%
R61M	5373	$4.35\ 10^{6}$	$5.40\ 10^{5}$	$4.67\ 10^{6}$	155.8%	7.0%

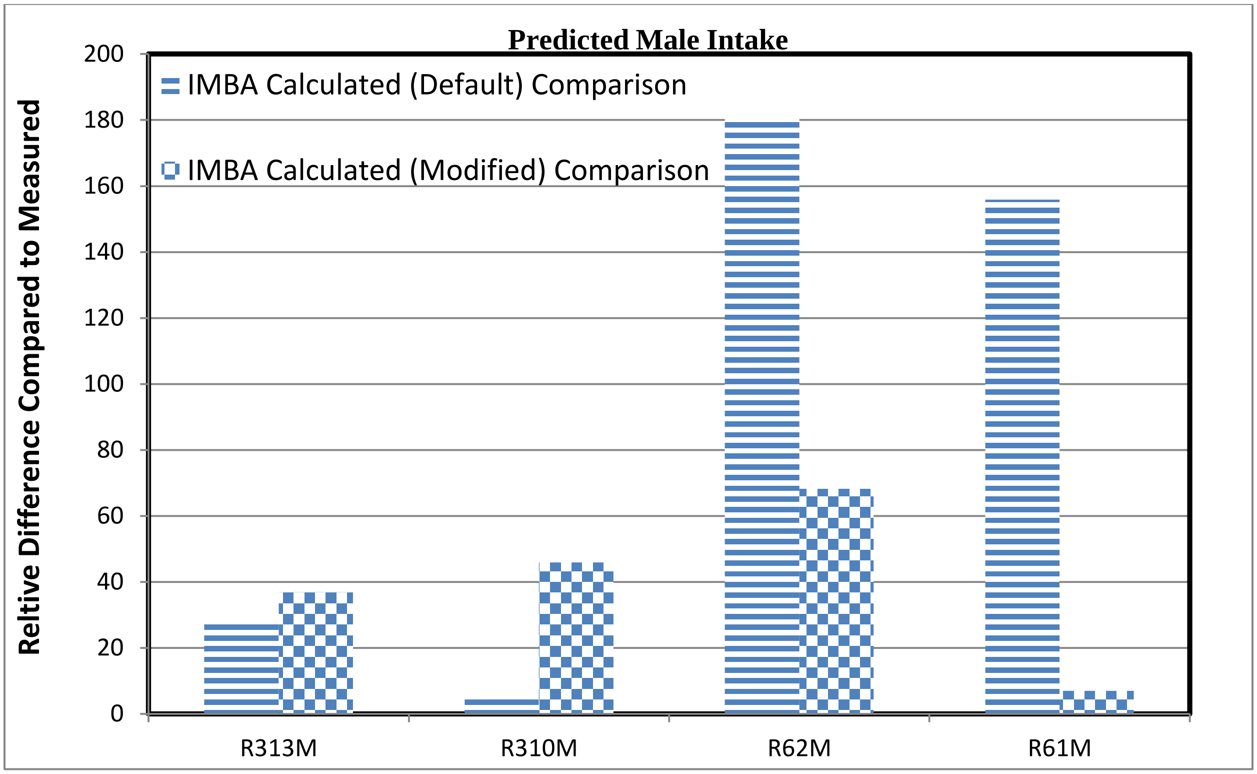

Figure 6.1 Comparison of Default and Optimized Male Model Intake Predictions in Independent Cases

Table 6.2 Independent Predicted Intake Comparison in Female Monkeys

Predicted Female Intake						
Case #	Time Post Injection	Injected Activity (Measured) (Bq)	IMBA Calculated (Default) (Bq)	IMBA Calculated (Modified) (Bq)	IMBA Calculated (Default) Comparison	IMBA Calculated (Modified) Comparison
R21F	6449	$1.83\ 10^{6}$	$4.09\ 10^{5}$	$2.45\ 10^{6}$	127.0%	28.9%
R32F	7168	$2.26\ 10^{6}$	$6.99\ 10^{5}$	$3.74\ 10^{6}$	105.4%	49.5%
R306F	14	$2.48\ 10^{6}$	$2.36\ 10^{6}$	$3.23\ 10^{6}$	5.0%	26.3%
R38F	3411	$1.85\ 10^{6}$	$1.27\ 10^{5}$	$9.07\ 10^{5}$	174.4%	68.6%
R39F	5650	$1.85\ 10^{6}$	$8.45\ 10^{4}$	$5.60\ 10^{5}$	182.6%	107.2%
R40F	99	$2.60\ 10^{6}$	$3.67\ 10^{5}$	$5.89\ 10^{5}$	150.6%	126.3%

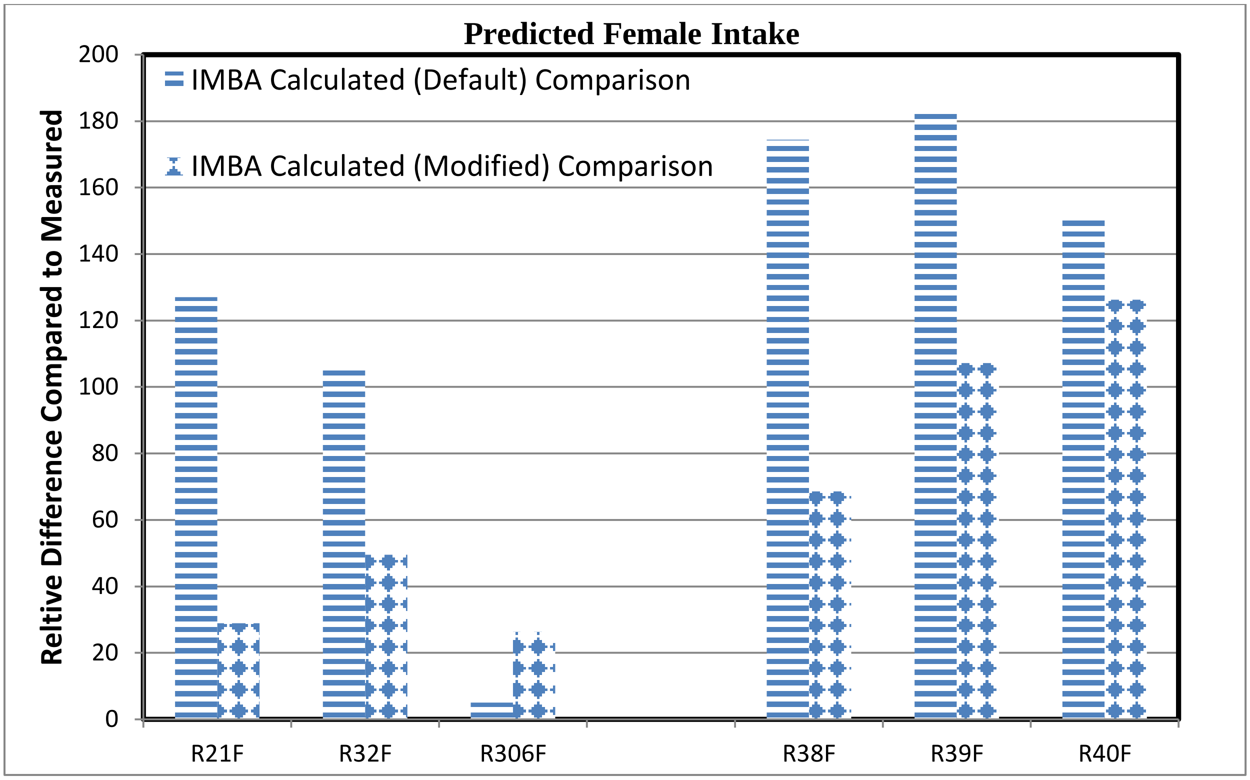

Figure 6.2 Comparison of Default and Optimized Female Model Intake Predictions in Independent Cases

Evaluating the male cases in Figure 6.1, it is evident that the optimized model parameters result in an improved model prediction in half of the cases. While the female test cases as shown in Figure 6.2 demonstrate an improved model prediction in all but one case R306F. Evaluating the difference in the data for the cases that were not improved by the optimized parameters, it is evident that these cases: R313M, R310M, and R306F all have a short time from injection to sacrifice. The reason for such a discrepancy is likely due to the fact the injected activity has not reached equilibrium.

Further evaluation of the test model indicates that the model did not include any short term to sacrifice cases (time to sacrifice < 500 days) in its creation.

The results of the optimized parameters, when comparing the activity in skeleton at death were somewhat mixed. When analyzing the predicted activity in skeleton for the male cases, we see an average improvement in all cases as shown in Table 6.3 and Figure 6.3, and all pass the criteria to be an improved model fit as stated in the hypothesis test, except R310M. However, not all female cases showed and improved prediction in the skeleton as shown in Table 6.4 and Figure 6.4. The majority, four out of six, (66.67%) however showed an improvement in the model prediction as defined in the hypothesis statement.

Table 6.3 Predicted Activity In Independently Evaluated Male Skeleton

	Predicted Male Skeleton					
	Time Post Injection	Injected Activity (Measured)	IMBA Calculated (Default)	IMBA Calculated (Modified)	IMBA Calculated (Default) Comparison	IMBA Calculated (Modified) Comparison
R313M	150	$4.60\ 10^{5}$	$8.15\ 10^{5}$	$3.38\ 10^{5}$	55.7%	30.4%
R310M	67	$2.11\ 10^{6}$	$8.30\ 10^{5}$	$8.46\ 10^{5}$	86.9%	85.4%
R62M	5853	$6.85\ 10^{4}$	$6.73\ 10^{5}$	$4.75\ 10^{4}$	163.1%	36.1%
R61M	5373	$1.08\ 10^{5}$	$5.31\ 10^{5}$	$4.17\ 10^{4}$	132.5%	88.5%

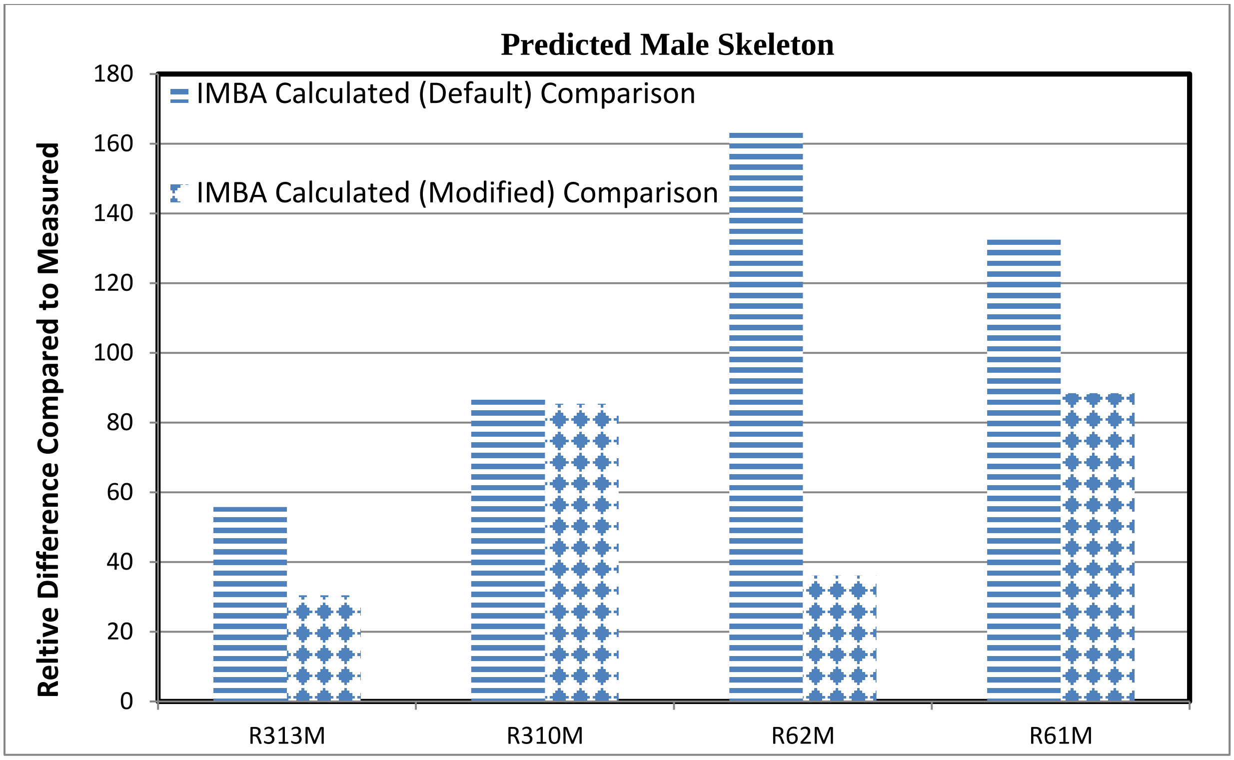

Figure 6.3 Relative Difference In Independent Evaluation of Male Skeleton

Table 6.4 Predicted Activity In Independently Evaluated Female Skeleton

Predicted Female Skeleton						
Case #	Time Post Injection	Injected Activity (Measured) (Bq)	IMBA Calculated (Default) (Bq)	IMBA Calculated (Modified) (Bq)	IMBA Calculated (Default) Comparison	IMBA Calculated (Modified) Comparison
R21F	6449	$7.82\ 10^{4}$	$1.71\ 10^{5}$	$7.02\ 10^{4}$	74.4%	10.8%
R32F	7168	$1.25\ 10^{5}$	$1.77\ 10^{5}$	$8.25\ 10^{5}$	34.6%	40.6%
R306F	14	$1.41\ 10^{6}$	$1.16\ 10^{6}$	$8.57\ 10^{5}$	19.4%	48.6%
R38F	3411	$4.00\ 10^{4}$	$3.78\ 10^{5}$	$8.79\ 10^{4}$	161.7%	74.8%
R39F	5650	$1.43\ 10^{4}$	$2.11\ 10^{5}$	$7.49\ 10^{4}$	174.6%	135.8%
R40F	99	$1.61\ 10^{5}$	$1.30\ 10^{6}$	$8.44\ 10^{5}$	155.9%	135.9%

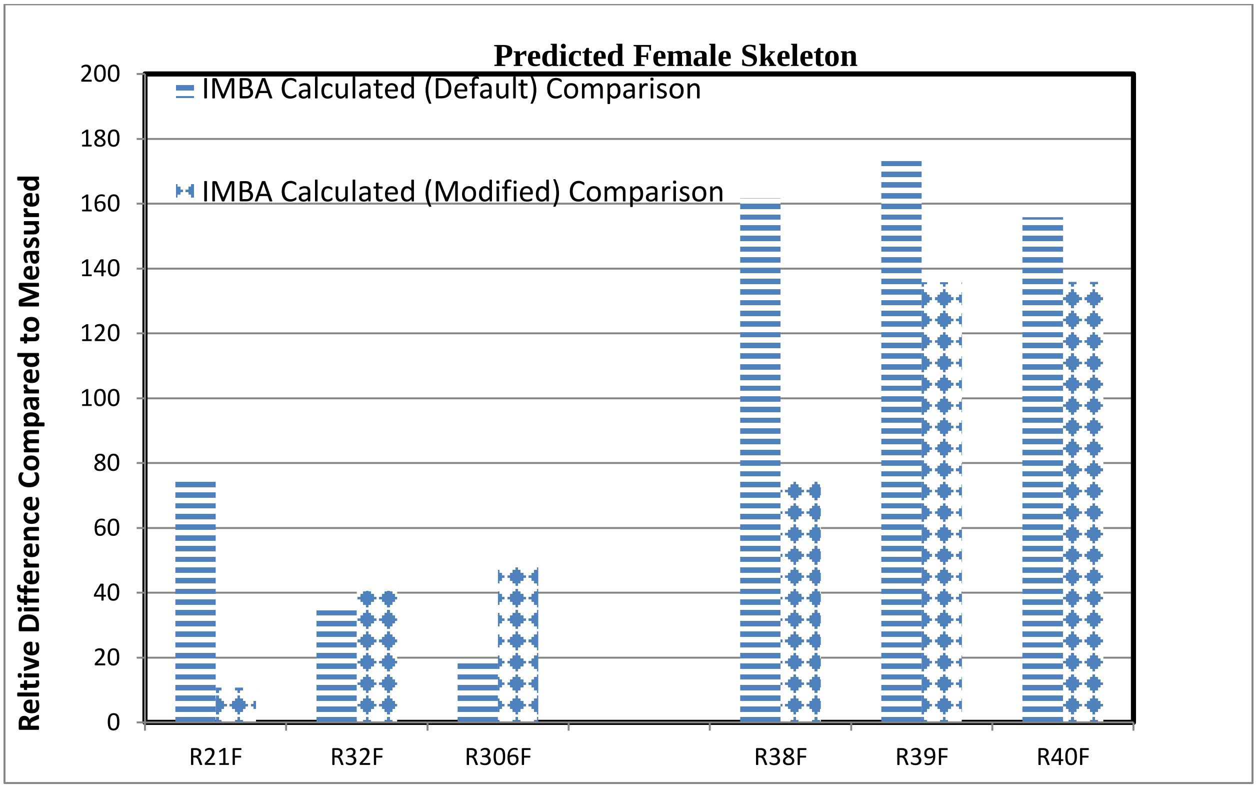

Figure 6.4 Relative Difference In Independent Evaluation of Female Skeleton

Chapter 7 SUMMARY AND CONCLUSIONS

7.1 Hypothesis Summary

In testing the robustness of the ICRP No. 78 ^{90}Sr systemic model, the systemic model did not accurately predict the intake from the composited primate bioassay data within 10%. The failure of the ^{90}Sr model to predict within 10% lead to the acceptance of the alternate hypothesis $H_{1,A}$. The support of the alternate hypothesis suggests that the intake prediction cannot be scrupulously predicted by the default ICRP No. 78 ^{90}Sr systemic model parameters.

Through altering the transfer rates for the Male and Female cohorts the predicted activity in skeleton was analyzed to determine if it was more accurate than the default predictions. For both the Male and Female sets of data, the alternate hypothesis $H_{2,A}$ was accepted such that the activities predicted in skeleton were 10% better than that of the default model. The acceptance of the alternate hypothesis advocates that the skeletal prediction can be improved by the altering of the default model parameters.

Through the testing of subjects independent of those used to optimize the default model, the predicted injected activity was compared between the default and optimized model. The majority of the cases both Male and Female showed a more accurate prediction than the default model by 10% or greater. This improvement in prediction can be used to predict the injected activity of subjects with similar injected activity, lead to the acceptance to the alternate hypothesis $H_{3,A}$. The acquiescence of the alternate hypothesis suggests that the intake prediction can be improved by the optimized model for the Male and Female test cases.

7.2 Summary and Conclusions

The default ^{90}Sr hermaphrodite systemic model produced a poor prediction of the activity injected using a maximum likelihood fit of the data for the composite monkey cohorts resulting in the acceptance of the alternate hypothesis. When evaluating the independent test cases, the model showed good predictions for subjects with short time to sacrifice. The discrepancies for the composite predictions and the majority of the independent test cases advocate that changes in the biokinetic parameters could improve the bioassay predictions.

The transfer of strontium in the bone compartment over time was the most essential in modeling to improve the predictive capabilities. The whole body counts were also very helpful in optimizing the model because they helped to directly quantify the activity residing in the body when data of the activity in skeleton was not available. However, the blood data in the modeling, and evaluating the independent subjects did not have as large of an effect due to the small quantities of activity contained within the samples. Nonetheless, the lower significance of the blood data did not decrease the predictive capabilities of the optimized model.

The prediction results of the modified model for both the male and female composite data sets were improved over that of the default parameters in favor of the second alternate hypothesis. The independent analysis of subjects not included in making the model also suggests an overall improved model prediction capability. The acceptance of the third alternate hypothesis test suggests this study can be used to predict the injected activity of other monkeys injected activity. The acceptance of all three alternate hypothesis suggest that the modified transfer rates could be used as default parameters for which further biokinetic modeling is completed using non-human primates as human surrogates.

7.3 Future Work

This study has illustrated the difficulty in specifying discrete parameters to describe the biokinetic transfer rates in a population that exhibits large natural variation in anatomy and physiology. Further analysis using known human cases should be evaluated to determine the models potential implementation as an improved model for human cases. The potential factors that may arise in such an analysis include the need for more subgroups to account for factors such as age and the background values that are present in the population. To gain knowledge on background radionuclides and there concentration in the skeleton, analysis of multiple cadavers should be conducted. A correlation between the activity in the known intake cases and the residual background can be determined to help quantify the intake over time.

REFERENCES

Ageyama, N. e. (2001, May). Specific Gravity of Whole Blood In Cynomolgus Monkeys, Squirrel Monkeys, and Tamarins. *Contemporary Topics in Laboratory Animal Science. Vol. 40, Issue 3* .

ATSDR. (2004). Toxicological profile for strontium. Atlanta, GA, United States. Retrieved from http://www.atsdr.cdc.gov/toxprofiles/index.asp

Birchall A, P. M. (2007). IMBA Professional Plus: A flexible approach to internal dosimetry. *Radiation Protection Dosimetry*, 194-197.

Birchall, & James. (1989). A microcomputer algorithm for solving first-order compartmental models involving recycling. *Health Physics*, 857-868.

Cember H, J. (2009). *Introduciton to Health Physics 4th Ed.* New York: McGraw Hill.

Doerfel H, A. B. (2006). *General guidelines for the estimation of committed effective dose from incorporation montitoring data*. Retrieved 2013, from htttp://ww.bologna.enea.it/attivita/ideas.html

Durbin PW, J. N. (1993a). *Collected original data on distribution of 90Sr in bones of monkeys.* Division of Life Sciences. Lawrence Berkely Laboratory.

Durbin PW, J. N. (1993b). *Collected original data on 90 Sr in plasma, whole body and excreta of monkeys.* Division of Life Sciences LBL.

Dzubay, S. (1975). Ambient air analysis with dichotomous sampler and x-ray fluorescence spectrometer. *Evironmental Science and Technology*, 663-668.

EPA, U. (2012, April 24). *Strontium.* Retrieved December 2013, from United States Environmental Protection Agency: http://www.epa.gov/radiation/radionuclides/strontium.html

Fraser R, H. M. (1960). The rate of calcium turnover in bone. Measurment by a tracer test using stable strontium. *Q J Med.*, 85-111.

Gibbs R, R. K. (2007). Evolutionary and Biomedical Insights from the Rhesus Macaque Genome. *Science*, 222-234.

Glasstone, & Dolan. (1977). The effects of nuclear weapons. *US Dept. of Defense and Dept. of Energy*, 653.

Gregersen MI, S. H. (1959). Cell volume, plama volume, totale blood volume and Fcells factor in the rhesus monkey. *American Journal of Physiology*, 184-187.

Hollrigl V, L. P. (2002). Studies of strontium biokinetics in humans. *Radiation Environment Biophysics*, 281-287.

ICRP. (1993). Age-dependent dose to members of the public from intake of radionclides: part 2, ingestion dose coefficients. *International commission on Radiological Prtection 23*. New York, New York: Pergamon Press.

ICRP. (1995a). 69. *International Commission on Radiological Protection Publication 69 Age Dependent dose to members of the public from intake of radionuclides: Part 3, ingestion dose coefficients*. New York, New York: Oxford: Elsevier Science.

IPS. (1995-2014). *International Primatological Society*. Retrieved 2014, from http://www.internationalprimatologicalsociety.org/

J, H., & P, D. (2008). Radiation Doses and risks from internal emiters. *Journal of Radiological Prtection*, 137-159.

Leggett, R. W. (1992). A Generic Age-Specific Biokinetic Model for Calcium-like Elements. *Radiation Protection dosimetry*, 183-198.

Luciani A, D. H. (2001). Sensitivity analysis of the urinary excretion of plutonium. *Radition Protection Dosimetry*, 179-183.

Malinovsky G, Y. I. (2013). Strontium Biokinetic modle for mouse-like rodent. *Journal of environmental Radioactivity*, 57-63.

Marsh JW, B. C. (2008). INternal Dose Assessments: Uncertainty studies and updat of IDEAS guidelines and databses within CONRAD project. *Raditon Protection Dosemetry*, 34-39.

Marsh, Y. S. (1998). A program for the comprehensive analysis of occupational cohort data. *Journal of Occupaitonal and Environmental Medicine*, 351-362.

Miller G, I. W. (2000). Analyzing bioassay data using Bayseing methods a primer. *Health Physics*, 512-518.

Miller G, M. H. (2002). Using exact Poisson likelihood funcitons in Bayesian interpretation of counting measurements. *Health Physics*, 598-613.

Mitruka, B. (1976). *Animals for medical research: models for the study of human disease.* New York: Wiley & Sons.

National, Research, & Council. (1997). *Chimpanzees in Research Stratigies for their ethical care managment and use.* Washington D.C.: National Academy Press.

Pogliani L. (1996). Matrix and convolution methods in chemical kinetics. *Journal of Mathmatical Chemistry*, 193-210.

Polig E. (2001). Modeling the distribution and dosimetry of internal emitters: A review of mathmatical procedures using matrix methods. *Health Physics* , 492-501.

Puncher, & Birchall. (2008). A Monte carlo method for calculating Bayesian uncertainties in internal dosimetry. *Radiation Protection Dosimetry*, 1-12.

Puncher, & Birchall. (2008). The autocorrelation coefficient as a tool for assessing goodness of fit between bioassay predicitons and measurment data. *Radiation Protection Dosimetry*, 370-373.

Sagine NB, T. E. (2003). Improvments in the biokinetic model for strontium with allowance for age and gender differences in bone mineral metabolism. *Radiaton Protection Dosimetry*, 619-622.

Skrable KW. (1974). A general equation for the kinetics of linear first-order phenomena and suggested applications. *Health Physics*, 155-157.

Sweet, V. L. (1993). Sources of toxic trace elements in urban air in Illinois. *Environmental Science and Technology*, 2502-2510.

Synhaeve N, S. J. (2011). Biokinetics of 90Sr after chronic igestion in a juvenile and adult mouse model. *Radiation Environmental biophysics*, 501-511.

Tanaka G, K. h. (1981). Distribution of strontium in the skeleton and in the mass of mineralized bone. *Health Physics*, 601-614.

Tolstykh EI, S. N. (2011). Does the cortical bone resorption rate change due to 90Sr-radiation exposure? analysis of data from Techa Riverside residents. *Radiaton Environmen Biophysics*, 417-430.

United States Environmental Protection Agency. (n.d.). Retrieved from http://www.epa.gov/radiation/radionuclides/strontium.html

U. S. DHS 2001 Toxicology profile for strontium: U. S. department of health and

human services. *Public health service agency for toxic substances and disease registry*

WHO. (2010). Strontium and Strontium Compounds. *World Health Organization Concise International Chemacal Assement Document 77*.

U. S. DHS 2001 Toxicology profile for strontium: U. S. department of health and human services. *Public health service agency for toxic substances and disease registry*